Quantitative Clinical Pharmacological Studies on Efavirenz and Atazanavir in The Treatment of HIV-1 Infection

Dinko Rekić

Department of Pharmacology
Institute of neuroscience and physiology
Sahlgrenska Academy at University of Gothenburg

UNIVERSITY OF GOTHENBURG

Gothenburg 2012

Cover illustration: Karin Dankis

Quantitative Clinical Pharmacological Studies on Efavirenz and Atazanavir in The Treatment of HIV-1 Infection

dinko.rekic@gu.se/dinko.rekic@gmail.com

ISBN 978-91-628-8590-8
http://hdl.handle.net/2077/29725

Printed in Gothenburg, Sweden 2012
Printer's name: Ale Tryckteam AB

Let my dataset change your mindset

Professor Hans Rosling

Quantitative Clinical Pharmacological Studies on Efavirenz and Atazanavir in The Treatment of HIV-1 Infection

Dinko Rekić

Department of Pharmacology, Institute of neuroscience and physiology
Sahlgrenska Academy at University of Gothenburg
Göteborg, Sweden

ABSTRACT

There are 34 million people infected with the HIV-1 virus in the world today. Due to increased access to antiretroviral therapy, AIDS related death has dropped by 30% since 2005. Optimizing the pharmacotherapy of the HIV-1 infection is of great importance to reduce adverse effects, reduce viral resistance development and increase the patients' survival as well as quality of life. This thesis presents pharmacometric applications to optimize pharmacotherapy of the HIV-1 infection as well as to expedite the clinical drug development of new drugs.

Methods to extrapolate *in vitro* data to *in vivo* settings have been applied to predict the level of the drug-drug interaction between efavirenz and rifampicin as well as to evaluate the current dosage recommendations. Nonlinear mixed effects (NLME) models, as implemented in the software NONMEM, have been fitted to data from clinical studies to investigate the disease effect of HIV-1 on efavirenz pharmacokinetics. Further, NLME modeling and simulation was used to evaluate and validate bilirubin as a marker of exposure and adherence in HIV-1 infected patients. Simulation of a mechanistic viral dynamics model, describing the interplay between virus and CD4 cells, was used to optimize the design and analysis of clinical trials in antiretroviral drug development. Model based techniques for hypothesis testing were shown to be superior in terms of power compared to traditional statistical hypothesis testing.

In conclusion, model based drug development techniques can be used to optimize HIV-1 therapy as well as expedite drug development of novel compounds.

Keywords: HIV, Pharmacokinetics, Pharmacodynamics
ISBN: 978-91-628-8590-8

SAMMANFATTNING PÅ SVENSKA

HIV är en virusinfektion som angriper celler viktiga för vårt immunförsvar. I dess slutgiltiga stadium, när immunförsvaret är nästintill fullständigt utslaget, övergår infektionen i tillståndet som betecknas som AIDS. Sett till antalet patienter är HIV/AIDS en sjukdom som främst drabbar de fattigaste delarna av världen. Av cirka 34 miljoner HIV-patienter i hela världen bor 23 miljoner i Afrika söder om Sahara.

Denna avhandling syftar till att förbättra användandet av de läkemedel som redan finns tillgängliga på ett sätt som är bättre anpassat till individen, s.k. individualiserad läkemedelsterapi. Förenklat säger man att det som läkemedlet gör med kroppen kallas *farmakodynamik* och det som kroppen gör med läkemedlet kallas *farmakokinetik*. Dessa två begrepp är således centrala i individualiseringen av läkemedelsbehandlingen och lika så i denna avhandling. Men hjälp av matematiska modeller beskrivs hur läkemedlet interagerar med kroppen dvs. vi kan beskriva både farmakokinetiken och farmakodynamiken. Dessa modeller kan vidare användas för att förklara varför vissa personer svarar framgångsrikt på en behandling medan andra inte gör det. Ibland kan denna skillnad förklaras av t.ex. genetiska faktorer eller andra läkemedel som orsakar ogynnsamma interaktioner. Genom att ta hänsyn till sådana faktorer kan man optimera behandlingen efter varje patients förutsättningar. Ett sådant exempel är interaktionen mellan HIV-läkemedlet efavirenz och tuberkulosläkemedlet rifampicin, där resultat från denna avhandling kan användas för att rekommendera hur mycket och för vem efavirenzdosen ska justeras för att undervika ogynnsamma effekter av interaktionen. Metodiken i detta arbete är av speciellt intresse då denna interaktion kunnat studeras i virtuella patienter i simulerade kliniska studier. På så sätt har anseenliga resurser och tid kunnat sparas. Detta är även av stor vikt för utvecklingen av framtida läkemedel då denna typ av studier är vanliga inom läkemedelsindustrin.

En annan frågeställning som har studerats är hur man ska övervaka så att patienter har tillräckliga läkemedelskoncentrationer i blodet. Nuvarande metodik kräver dyr laboratorieutrustning som ofta saknas i länder svårast drabbade av HIV/AIDS. Med hjälp av modeller har en kroppsegen substans, bilirubin, som kraftigt reagerar på närvaro av HIV-läkemedlet atazanavir kunnat användas som en indikator på adekvata läkemedelskoncentrationer i blodet. Bilirubin är mycket enkelt att mäta utan dyr utrustning. Resultaten i studien har kunnat bekräftas i 222 patienter från Italien, Frankrike och Norge.

Sammanfattningsvis kan resultat från denna avhandling förbättra vården av HIV/AIDS patienter genom att optimera deras behandling, även i de fattigaste delarna av världen. Vidare har resultaten visat nyttan av användandet av modeller inom läkemedelsforskning som kan vara av gagn för läkemedelsindustrin.

LIST OF PAPERS

This thesis is based on the papers listed below, which are referred to in the following text by their Roman numerals.

I. Rekić D, Röshammar D, Mukonzo J, Ashton M. In silico prediction of efavirenz and rifampicin drug–drug interaction considering weight and CYP2B6 phenotype. British Journal of Clinical Pharmacology. 2011; 71 (4):536–43.

II. Mukonzo JK[1], Nanzigu S[1], Rekić D, Waako Paul, Röshammar D, Ashton M, Ogwal-Okeng J, Gustafsson LL, Aklillu E. HIV/AIDS patients display lower relative bioavailability of efavirenz than healthy subjects. Clinical Pharmacokinetics. 2011; 50 (8):531–40.

III. Rekić D, Clewe O, Röshammar D, Flamholc L, Sönnerborg A, Ormaasen V, Gisslén M, Äbelö A, Ashton M. Bilirubin-a potential marker of drug exposure in atazanavir-based antiretroviral therapy. The AAPS journal. 2011 Sep 13; 13 (4):598–605.

IV. Rekić D, Röshammar D, Bergstrand M, Tarning J, Calcagno A, D'Avolio A, Ormaasen V, Vigan M, Barrail-Tran A, Ashton M, Gisslén M, Äbelö A. External validation of the bilirubin-atazanavir nomogram for assessment of atazanavir plasma exposure in HIV-1 infected patients. Submitted

V. Rekić D, Röshammar D, Simonsson USH. Model based design and analysis of phase II HIV-1 trials. Submitted

Reprints were made with kind permission from respective publisher

[1] Equal contribution

CONTENT

ABBREVIATIONS

AIDS	Acquired immunodeficiency syndrome
ARV	Antiretroviral
AUC	Area under the concentration-time curve
CD4	Helper T lymphocyte
CI	Confidence interval
CL	Clearance
CL_{int}	Intrinsic clearance
CV	Coefficient of variation
CYP	Cytochrome P450
EC_{50}	Concentration required to achieve 50% of maximal drug response
E_{inh}	Inhibitory drug response
EM	Extensive metabolizer
Eq	Equation
F	Bioavailability
FDA	(US) Food and Drug Administration
FOCE-I	First-order conditional estimation
fu	Fraction unbound drug in plasma
HAART	Highly active antiretroviral treatment
HIV	Human immunodeficiency virus
IC50	Concentration required to achieve 50% of maximal inhibition
IIV	Interindividual variability
IPRED	Individual prediction
ka	Frst-order absorption rate constant
k_{in}	Zero-order production rate constant
k_{out}	First-order removal rate constant
LW	Liver weight
MPPGL	Milligram protein per gram liver
NNRTI	Non-nucleoside reverse transcriptase inhibitor

NRTI	Nucleoside reverse transcriptase inhibitor
OFV	Objective function value
PD	Pharmacodynamics
Pgp	P-glycoprotein
PI	Protease inhibitor
PK	Pharmacokinetics
PM	Poor metabolizer
PRED	Population prediction
Q	Inter-compartmental clearance
QD	*Quaque die* (lat.) every day or daily
Q_H	Hepatic blood-flow
R	Viral reproduction ratio
RNA	Ribonucleic acid
RSE	Relative standard error
SD	Standard deviation
SNP	Single nucleotide polymorphism
TB	Tuberculosis
V	Volume of distribution
V_c	Central volume of distribution
V_p	Peripheral volume of distribution
VPC	Visual predictive check
WHO	World Health Organization
ε	Residual variability: difference between individual predictions and observations
η	Interindividual variability: difference between typical and individual parameter estimate
θ	typical parameter value

DEFINITIONS IN SHORT

Pharmacokinetics (PK)	What the body does to the drug (1).
Pharmacodynamics (PD)	What the drug does to the body (1).
Population pharmacokinetics (popPK)	The study of the sources and correlates of variability in drug concentrations among individuals who are the target patient population receiving clinically relevant doses of a drug of interest (2).
Pharmacometrics	Branch of science concerned with mathematical models of biology, pharmacology, disease, and physiology used to describe and quantify interactions between xenobiotics and patients, including beneficial effects and side effects resultant from such interfaces (3).

1 INTRODUCTION

This thesis focuses on quantitative clinical pharmacology as a method to improve antiretroviral pharmacotherapy used in the treatment of the HIV-1 infection. In quantitative clinical pharmacology one objective is to quantify the determinants of drug exposure in man, the relationship between drug exposure and response as well as adverse and therapeutic outcomes. It has been said that pharmacometrics is the science of quantitative clinical pharmacology is (4). The main tool of pharmacometrics is nonlinear mixed effects (NLME) modeling. In NLME modeling, processes related to disease and drugs are represented by mathematical equations. A broader definition of pharmacometrics can be found in the definitions section on page (vii).

The five Papers in this thesis deal with fundamental questions in clinical pharmacology such as how drug-drug interactions should be studied or predicted (Papers I and II), development and validation of biomarkers (Papers III and IV) and implementations of model based drug development in design and analysis of clinical trials (Papers V). The findings in this thesis are thus equally important to the optimization of HIV-1 therapy as to clinical drug development in general.

The chapters in this thesis are organized as follows. Chapter 1 gives a brief introduction to the fundamentals of HIV-1 infection and its pharmacotherapy with special emphasis on the role of the drugs investigated in this thesis (efavirenz and atazanavir). Chapters 2 and 3 provide some background for Papers I-IV. Chapter 4 serves to familiarize the reader to the pharmacometric tools and their use in clinical pharmacology. Two approaches are introduced and discussed, a) *In vitro-in vivo* extrapolation and b) nonlinear mixed effect modeling. The use of model based hypothesis testing is also introduced in Chapter 4 along with some background to Paper V

The five papers are condensed into five specific questions that this thesis aims to answer. These questions are listed in Chapter 5. The methods, results and the discussion of individual papers are addressed in Chapters 6, 7 and 8, respectively, while general conclusions from the investigations in this thesis are presented in Chapter 9.

1.1 The HIV/AIDS epidemic

According to the Global HIV/AIDS response progress report, 2.7 million people became infected with HIV-1 in 2010 (5). Although a decline in numbers from the year before it is a substantial addition to the 34 million people infected with HIV worldwide. Increased availability of highly active antiretroviral treatment (HAART) has resulted in a global decrease in deaths related to AIDS. This trend is most apparent in sub-Saharan Africa where AIDS related death has decreased by 30% since 2005 (5). Although this represents a positive trend, it is estimated that only 47% of eligible patients receive HAART treatment in low and middle income countries rendering AIDS as one of the largest causes of death in sub-Saharan Africa (5) (Figure 1).

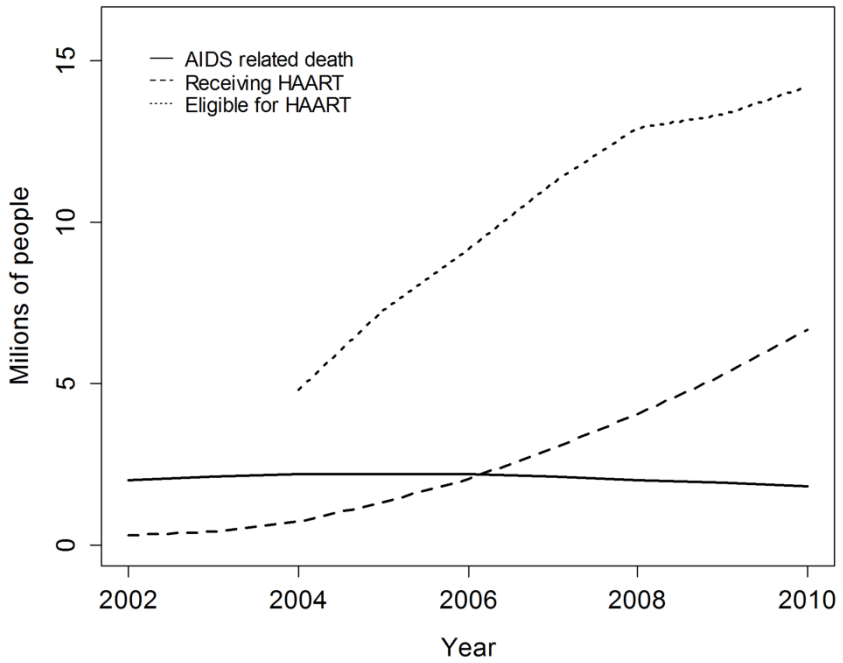

Figure 1. Number of people eligible for highly active antiretroviral treatment (HAART), dying from AIDS related causes and number of people receiving HAART versus time. A decrease in AIDS related death is observed after 2005, due to increased availability of HAART(5).

1.2 Principles of antiretroviral therapy

The pharmacotherapy of HIV infection is perhaps best described through the viral infection and replication cycle (Figure 2). Virus enters the human body through exchange of bodily fluids. While routes of transmission vary between different geographical, cultural and economic regions of the world, common transmission routes include; unprotected vaginal and anal intercourse, sharing of contaminated needles during recreational drug use and mother to infant transmission (prenatal or postpartum trough breast feeding). Mother to infant transmission is particularly common in sub-Saharan Africa (5,6).

During transmission, HIV binds to immune cells expressing the CD4 receptor (monocytes, macrophages and T-cell lymphocytes). Co-receptors (CCR5, CXCR-4) interact with viral receptors gp120 and gp41 causing conformational changes allowing the virion to fuse with the host cell (7,8). This interaction is the main target for entry/fusion inhibitors. Currently only two drugs are approved in this class and although both drugs prevent entry/fusion of the virus they act on different targets. Enfuvirtide, binds to the gp41-gp120-CD4 receptor complex preventing fusion of the viron with the host cell while maraviroc is a CCR5 receptor antagonist (9,10). Enfuvirtide is a peptide hence only available for intravenous administration (9). Maraviroc is currently the only drug not targeting the virus directly but instead blocking the virus' access to the host cell. HIV that is CXCR-4 tropic or dual tropic is consequently not affected by maraviroc (10).

After successful fusion with the host cell the virion releases its content of viral RNA and several viral enzymes including reverse transcriptase (RT), integrase, ribonuclease and protease (7,8). The viral RNA is transcribed into complementary DNA (cDNA) by RT. This step in the viral lifecycle poses one of the main targets of antiretroviral drugs.

Nucleoside and nucleotide reverse transcriptase inhibitors (NtRTI and NRTI) are pro-drugs that are activated by the host cell through phosphorylation. When activated they are structural analogs to endogenous deoxynucleoside triphosphates (dNTP) lacking the 3´-OH group necessary to form the 3´-5´ phosphodiester bond between the dNTP. This effectively leads to termination of reverse transcription (11). This class of drugs constitutes the background therapy in HAART.

Non-nucleoside reverse transcriptase inhibitors (NNRTI) are allosteric inhibitors of reverse transcriptase. Efavirenz is one of the first developed NNRTI and is currently recommended as an option for first line therapy. NNRTs are only effective against HIV-1 because of the virus-strain specific binding site to RT (12) and, like all NNRTIs, efavirenz is sensitive to mutations in the allosteric site of reverse transcriptase (11,13). A single change in amino-acid sequence is enough to develop resistance. Monotherapy with NNRTIs can lead to resistance within a few days or weeks (14).

After transcription, cDNA and its complement forms double-stranded viral DNA that is transported into the nucleus. Inside the nucleus, the viral enzyme integrase integrates the viral DNA into the host genome (7). This step is the target of the integrase inhibitor raltegravir which inhibits the integration by binding to the integrase-DNA complex. Presence of viral DNA is hence necessary for the drug effect (15). The virus remains latent in the genome until activated by transcription factors. Once activated, viral RNA and proteins are produced. The viral envelope and viral proteins are assembled near the cell membrane (8). Assembled virus are pinched of the cell membrane in a process known as budding (16).

During budding or short after, new virus matures trough cleaving of Gag and GagPol polyprotein precursors into mature Gag and Pol proteins. This process is mediated by viral protease and is the target for protease inhibitors (PI). PIs like atazanavir effectively stop the viral maturations process, resulting in production of non-infections virus (16). Protease inhibitors can stop production of infectious virus regardless of a cells' infection stage. While reverse transcriptase inhibitors (NNRTI, N(t)RTI) and integrase inhibitors can protect newly infected cells from becoming latently infected, they provide no benefit to cells already producing new virus (17).

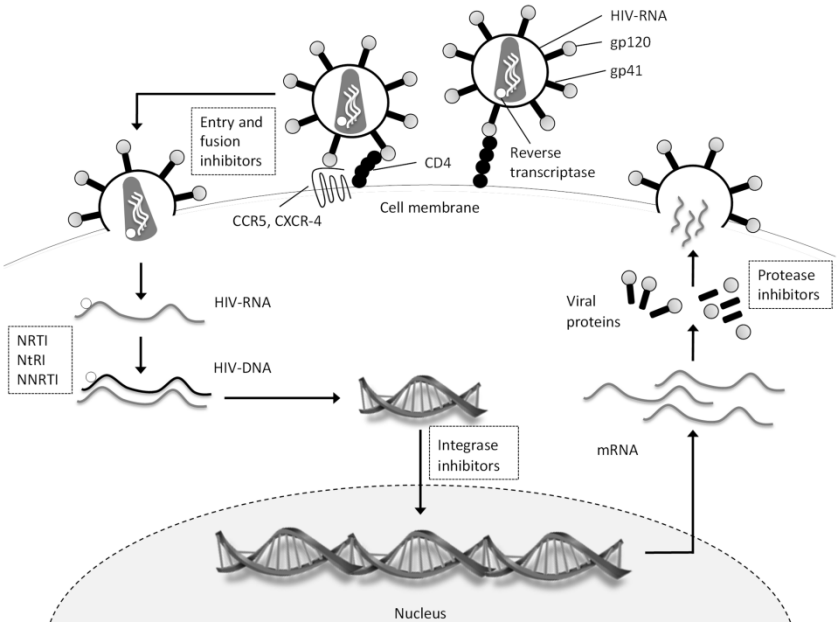

Figure 2. Viral replication cycle of HIV-1 with the sites of action for available antiretroviral agents indicated by the white boxes.

1.3 Therapy goals

Treatment is generally recommended in all patients with an AIDS-defining illness or if the CD4 cell count reaches below 350 cells/mm^3 (18). Eradication of the infection has so far not proven feasible due to the longevity of latently infected CD4 cells. Thus, current treatment goals of antiretroviral therapy are, in addition to prevent transmission, to reduce the morbidity and increase the duration of survival and quality of life (18). To achieve these goals it is necessary to reach minimal HIV levels in plasma for as long time as possible. This is usually achieved by combination therapy after the during 12-24 weeks of treatment. Optimal viral suppression is defined as viral loads below the level of detection for the assay, usually <20-75 copies/mL (18). Combinational therapy of 2 NRTIs with a PI or NNRTI are recommenced for most patients (13,19) Currently, adherence difficulties are believed to be the main reason for low therapy success rate (19). Although, with the introduction of ritonavir boosted PI therapy and the NNRTIs adherence rates of >95% are no longer required for viral suppression. Moderate adherence rates have been shown to result in successful viral suppression in most patients (19).

1.4 The role of efavirenz and atazanavir/r

Efavirenz was the first NNRTI approved for once daily dosing resulting in a decreased pill burden for patients. Efavirenz is the preferred choice of NNRTI for combination therapy, except in pregnant women during the first trimester (20). Efavirenz based regimens are frequently used in resource limited settings due to convenient administration, effectiveness and long-term tolerability. No other regimen has produced better long term treatment response in randomized clinical trials (18,20). Sufficient virological suppression can be achieved with lower degree of adherence with efavirenz and other NNRTI regiments than with protease inhibitors (21). This is attributed to the longer elimination half-life of NNRTI compared to PIs (21).

Up to 55% of patients on an efavirenz based regimen experience CNS side effects during the first 2-4 weeks of therapy. Commonly occurring side effects include: dizziness, insomnia, impaired concentration, agitation, amnesia, abnormal dreams and hallucinations (22). Generic efavirenz regimens are available in resource limited settings at an affordable cost. In 2010 the price for a year's supply of an efavirenz-containing first line regimen for one person was less than 100 USD, a 50% decrease in price from 2008 (5). Reasonable pricing, alongside the proven long term efficacy and safety, make efavirenz a popular treatment in resource limited settings.

In contrast to efavirenz, atazanavir remains unavailable for the vast majority of patients. It is estimated that 8% of newly infected patients in USA carry NNRTI resistant HIV (23), while virus resistant to PIs is rarely observed in pa-

tients with virological failure (24). Protease inhibitors are thus an important alternative and atazanavir is one of the preferred PIs in combinational therapy (25). Protease inhibitors are frequently administered with ritonavir which acts as a pharmacokinetic booster, inhibiting mainly gastric CYP3A4, the main metabolizing enzyme of PIs, resulting in increased bioavailability of PIs (26). Atazanavir, boosted with ritonavir is available for once daily dosing resulting in a lower pill burden for patients. The main adverse effect of atazanavir is hyperbilirubinemia, but this is rarely a cause for treatment discontinuation (25).

2 PHARMACOKINETICS AND PHARMACODYNAMICS OF EFAVIRENZ

Efavirenz is generally well absorbed, reaching peak plasma levels between three to five hours after oral dosing. Oral bioavailability is slightly increased by fatty meals while the liquid formulations have lower bioavailability compared to tablets/capsules (27). An increase in efavirenz exposure due to fatty food has been confirmed in Ugandan patients (28). Efavirenz is highly bound to plasma proteins, mostly albumin (>99%), with a relatively long half-life (40-55 h) at steady state (27). The long half-life allows once daily dosing which is thought to result in better patient compliance (21).

2.1 Efavirenz *in vitro* and *in vivo* metabolism

Efavirenz is mainly eliminated through hepatic metabolism (29). The two main metabolites found in plasma are 8-hydroxy-EFZ and 7-hydroxy-EFZ which are believed to account for 77.5 and 22.5 % of the overall efavirenz metabolism, respectively (30–32). The main mediator of the 8-hydroxy pathway is CYP2B6 with minor contributions from CYP1A2, CYP3A4, CYP3A5 and CYP2A6, while the 7-hydroxy pathway relies on CYP2A6 (31,32). *In vitro* data also identifies CYP1A6 as a small contributor to efavirenz metabolism (31). A 8,14-hydroxy-EFZ metabolite has also been identified *in vitro* and *in vivo* (29–31). It has been suggested that the 8,14-dihydroxy-EFZ metabolite is formed by secondary oxidation of the 8-hydroxy-EFZ metabolite by CYP2B6 (30,31) although new investigations have failed to confirm these findings (32). All three hydroxy metabolites are excreted in the urine mainly as glucuronide conjugates and to a lesser extent as sulphate conjugates (30). It appears that there is no specific uridine 5'-diphospho-glucuronosyltransferase (UGT) that is responsible for glucuronidation of the hydroxy metabolites but instead a barrage of UGT enzymes with unknown individual contribution (33). To a small extent efavirenz is directly conjugated by UGT2B7 to form EFZ N-glucuronide (30,31,33). Efavirenz exhibits profound auto-induction of CYP2B6 and to a lesser degree of CYP3A4 (34,35). The metabolic pathways of efavirenz are depicted in Figure 5.

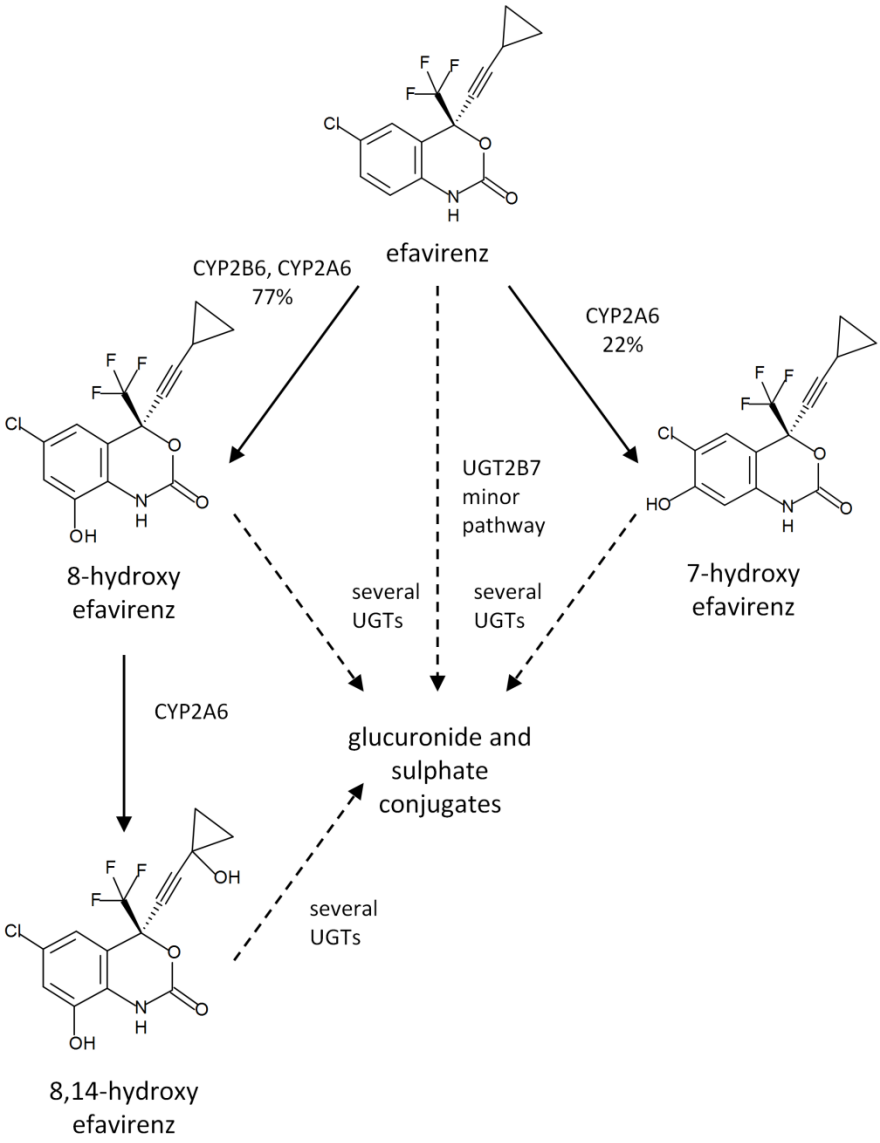

Figure 3. Proposed metabolic pathways of efavirenz and its metabolites, based on *in vitro* incubations. References and explanations to abbreviations can be found in section 2.1 of chapter 2.

2.2 Efavirenz pharmacogenetics

Efavirenz displays large interindividual pharmacokinetic variability that is often attributed to the highly polymorphic CYP2B6 enzyme. Several single nucleotide polymorphisms (SNPs) have been shown to influence the oral clearance (CL/F) of efavirenz. Most predominant is the CYP2B6*6 516G→T single nucleotide polymorphism which has been associated with a 21% lower CL/F after a single dose and up to 75% lower CL/F at steady state in homozygous subjects (36–39). Also the 983T→G and 785A→G SNPs have been shown to increase efavirenz plasma concentrations (38,40,41). Polymorphism in the CYP2B6 enzyme is unevenly distributed among different populations. The highest frequency of the 516G→T allele is observed in Africans (45.5%) while its spread in the European and Asian populations is substantially lower, 21.4 and 17.4%, respectively (42,43). In some African populations frequencies of the 516G→T allele are observed in up to 71% of the subjects (39).

Efavirenz pharmacokinetics has also been shown to be affected by genetic variation in the adenosine triphosphate-binding cassette, sub-family B, member 1 (ABCB1) gene coding for P-glycoprotein (38,40). However, there is some disagreement about the importance of P-glycoprotein to efavirenz pharmacokinetics (44).

Arab-Alameddine *et al.* showed the importance of SNP 17163G3T of CYP3A4 to CL/F in patients with impaired CYP2B6 (45). Also CYP2A6 along with UGT2B7 polymorphisms have been shown to influence CL/F (46), most notably in CYP2B6 poor metabolizers (45).

2.3 Influence of rifampicin on efavirenz pharmacokinetics

HIV infected patients are frequently co-infected with tuberculosis (47). Despite the potential to induce several cytochrome P450s, rifampicin is commonly used in the treatment of tuberculosis infected HIV-1 patients in Africa. Rifampicin is a known inducer of CYP1A2, CYP2B6, CYP2C19, CYP2C8, CYP2C9 and CYP3A (48,49).

Rifampicin has been shown to reduce the area under the concentration-time curve (AUC) of efavirenz by 22% (50). Although this decrease in efavirenz exposure is unlikely to be of any clinical significance (51) the question whether the efavirenz dose should be increased in presence of rifampicin has been raised and is supported in most guidelines (25). A weight-based cutoff for the dose increment has been suggested by the US Department of Health and Human Services (25). Moreover, in a recent FDA case study, further clinical trials or *in silico* simulations were encouraged to explore the need of a dose increment (52). Recently, some contradicting results have been published, showing inverse effect

on efavirenz kinetics by rifampicin resulting in an increase of efavirenz exposure (53). These findings remain yet to be explained.

2.4 Disease effect on efavirenz pharmacokinetics

The pharmacokinetics of drugs are governed by a number of physiological processes that may or may not be affected by the HIV-1 infection. Conclusions from drug-drug interaction studies or other Phase I studies conducted in healthy volunteers may therefore not always be transferable to patients. Several examples of drug-drug interaction studies in healthy volunteers where efavirenz is the main perpetrator are available in the literature (54–59). A possible difference in pharmacokinetics between patients and healthy volunteers entails a risk for confounding results from such clinical trials. Furthermore, the traditional phase I trials in clinical drug development are conducted in healthy volunteers which may give misleading information on drug exposure in the target population, in this case HIV-1 patients.

Difference in CYP activity between HIV-1 patients and healthy volunteers has been shown for a number of CYP-isoforms. Recently, Jetter *et al.* showed a 50% reduction in CYP3A4 activity in HIV-1 infected patients compared to healthy volunteers when administering the CYP3A4 probe drug midazolam. (60). Jones *et al.* observed 90% decreased CYP2D6 activity in HIV-1 infected patients compared to healthy volunteers (61). These findings are supported by animal and *in vitro* studies that showed altered cytochrome P450 and transporter protein activity associated with infection and inflammation. These changes appear to be mediated trough inhibition/destabilization/modulation of cytokine expression by nitric oxide (60,62–64).

In addition to changes in CYP-mediated metabolism, HIV-1 infected patients have been shown to have elevated and highly variable gastric pH (65). This may affect the pharmacokinetics of some protease inhibitors known to have pH dependent absorption (66). Atrophy and/or blunting of the absorptive surface for drugs in the gastrointestinal tract may also affect pharmacokinetics of some antiretroviral drugs due to decreased rate and/or extent of absorption (67,68).

HIV-1 infection is associated with elevated alpha 1-acid glycoprotein, while HIV-related wasting syndrome leads to decreased albumin levels (69,70). Changes in plasma protein concentration are not expected to alter unbound drug concentrations, they may, however, lead to altered total plasma concentrations which can increase variability and lead to misinterpretation of plasma concentration measurements.

2.5 Efavirenz exposure response relationship

The concentration response relationship of efavirenz is not well characterized. However, there appears to be a consensus concerning the therapeutic window of efavirenz.

Marzolini *et al.* investigated 130 HIV-1 infected patients whose plasma concentrations were sampled on average (SD) 14 (±2.7) hours after dosing. Ten patients were found to have plasma exposure below 1 mg/L, five of these patients experienced viral failure during the study. Four out of seventeen patients with plasma concentrations over 4 mg/L experienced severe central nervous system (CNS) adverse events (71), including dizziness, nausea, headache, fatigue, insomnia and vomiting (27,71). Plasma concentrations versus presence of CNS adverse events as well as virological failure was analyzed with logistic regression (71). It was concluded that patients with plasma concentrations below 1 mg/L had a higher probability of virological failure compared to those with higher plasma concentrations, while patients with plasma concentrations above 4 mg/L had higher probability of CNS adverse effects. Similar findings have been observed in other studies (72–74).

3 PHARMACOKINETICS AND PHARMACODYNAMICS OF ATAZANAVIR

3.1 Atazanavir pharmacokinetics

Ritonavir boosted atazanavir (atazanavir/r) is rapidly absorbed reaching peak plasma concentrations two hours after oral absorption (75,76). The extent of absorption is highly dependent of pH as well as food intake. Daily intake of the proton pump inhibitor omeprazole (20 mg daily) has been shown to reduce atazanavir AUC by 42% (66) while atazanavir administration with a light meal increased the atazanavir AUC by 70% (76,77). Atazanavir is 89% bound to α_1-acid glycoprotein (AGP) and 86% to albumin (76). Similarly to other protease inhibitors, atazanavir is mainly metabolized by CYP3A4 (75–78). Following a 400 mg dose, it is estimated that 20% and 7% of the drug is recovered unchanged in feces and urine, respectively (77). In a population pharmacokinetic study CL/F and V/F were estimated to 7.7 L/h and 103 L respectively, resulting in an elimination half-life of 9.27 hours (75).

3.2 Bilirubin

Bilirubin is the degradation product of hemoglobin which is released from damaged or old erythrocytes. Hemoglobin is phagocytized by Kupffer-cells in the reticulo-endothelial system of the spleen, liver and bone marrow (79). The degradation product, bilirubin, is released into the plasma, where it is highly bound to albumin. In the liver, unconjugated bilirubin is transported across the hepatocyte cell membrane by the organic anion- transporting polypeptide 1B1 (OATP–1B1. Passive diffusion is also believed to be of importance (80,81). In hepatocytes, mono- and diglucuronide are formed by glucoronidation of bilirubin by UGT1A1 (82).

Gilbert's syndrome is caused by an inherited variation in the promoter region or the gene of the UGT1A1 enzyme resulting in reduced amounts of normal protein and mildly elevated levels of unconjugated bilirubin i.e. hyperbilirubinemia. Several variants of the UGT1A1 gene or promoter region are associated with Gilbert's syndrome of which UGT1A1*28 is believed to be the most common. Gilbert's syndrome affects approximately 10% of the Caucasian population (83).

Bilirubin glucuronides are transported by multi-drug resistance protein 2 (MRP–2) into the hepatic canaliculi (79). Bilirubin is deconjugated and degraded by bacterial enzymes to form urobilinogen in the colon. A small amount of uro-

bilinogen is reabsorbed only to be recirculated by the liver or excreted by the kidneys. Unreabsorbed urobilinogen is further metabolized into urobilin and stercobilin and excreted in the feces (79)

3.3 Atazanavir induced hyperbilirubinemia

Hyperbilirubinemia is commonly observed in patients on an atazanavir/ritonavir based antiretroviral treatment, although it is an uncommon cause of treatment discontinuation (25). The hyperbilirubinemia is attributed to a concentration-dependent atazanavir inhibition of UGT1A1 (84). UGT1A1 gene allele*28 has been associated with increased risk of hyperbilirubinemia in several studies (85,86).

Recent work has, however, revealed a complex interplay between multiple transporters, affecting both atazanavir and bilirubin. Atazanavir has been shown to be an inhibitor and a substrate of several OATPs, including 1B1, responsible for part of the bilirubin transport into the hepatocyte (80,81,87). Although the role of OATP1B1 may not be clear it seems to be of importance for bilirubin elevation and possibly atazanavir exposure (88). This has led to discussion on which mechanism is most important for the atazanavir-induced hyperbilirubinemia (89). The enzymes and transporters involved are depicted in Figure 4.

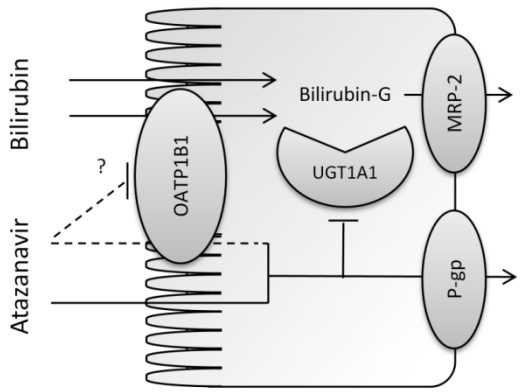

Figure 4. Illustration of the bilirubin elimination process by the hepatocytes and the suggested associated proteins and transporters. Bilirubin can enter the hepatocytes passively (diffusion) and actively trough the organic anion-transporting polypeptide (OATP) 1B1. Bilirubin glucuronidation is mediated by glucuronosyltransferase (UGT) 1A1. The bilirubin glucuronide is excreted into bile canaliculi by multi-drug resistance protein (MRP) 2. Atazanavir is thought to enter the hepatocytes passively and to some extent actively by OATP1B1. Atazanavir inhibits UGT1A1 and possibly OATP1B1. Atazanavir is a also substrate for p-glycoprotein (P-gp).

3.4 Atazanavir exposure response relationship

The suggested minimum effective concentration (MEC) for atazanavir is 150 ng/mL or 0.2 µmol/L (18). These recommendations are based on logistic regression of plasma trough concentration and virological outcome at week 28 of therapy in 51 patients (90). At week 28 of treatment, 37.5% of patients with atazanavir concentrations below 0.2 µmol/L were reported to achieve viral suppression in comparison to the 81% of patients with atazanavir concentrations >0.2 µmol/L who achieved viral suppression (90).

3.5 Bilirubin as a marker of atazanavir exposure

Patients with successful virological suppression on atazanavir monotherapy have significantly higher bilirubin elevations than those failing the treatment (91). Similar direct relationships between atazanavir concentrations and virological outcome have not been demonstrated (91). This has led to suggestions that bilirubin may be used as a marker of adherence to atazanavir therapy and possibly therapeutic outcome (91–95). Petersen *et al.* identified bilirubin to have 87% sensitivity and 63% specificity for prediction of adherence (92). In that study, adherence was measured in terms of viral suppression. Patients with successful suppression were deemed adherent to therapy while those with unsuccessful suppression were classified as non-adherent (92). An increase in bilirubin concentration from baseline by 6.84 µmol/L predicted viral suppression with a negative predicted value (NPV) and positive predicted value (PPV) of 68% and 86%, respectively. These finding have yet to been confirmed in an external patient population.

Although not routinely recommended, therapeutic drug monitoring (TDM) of atazanavir have in some cases shown to improve the ARV therapy (96). Other studies have, however, failed to show any benefit (94). The widespread use of TDM may in part be hindered by the cost of analytical equipment and availability of skilled personnel needed to operate and maintain the equipment. These obstacles are largely diminished by the high availability, low cost and simplicity of bilirubin assays.

4 PHARMACOMETRIC TOOLS IN CLINICAL PHARMACOLOGY

4.1 Impact of pharmacometrics in therapy optimization and drug development

Pharmacometrics is the science of quantitative clinical pharmacology (4). It utilizes mathematical models to quantify the interaction between the xenobiotics and humans. Pharmacometrics as part of a model based drug development program can reduce size, cost and failure rate of clinical trials (97,98). Pharmacometrics plays an increasing role for support of labeling and approval decisions at the U.S. Food and Drug Administration (FDA). Between 2000 and 2008 the pharmacometric reviews at FDA were estimated to influence the approval and labeling decision in 64% and 67% of cases, respectively (99).

Pharmacometrics is also gaining recognition for optimization of therapies for a variety of poverty related diseases, including but not limited to malaria, tuberculosis, human African trypanosomiasis and HIV-1.

Nonlinear mixed effects (NLME) modeling is the most important tool of pharmacometrics. NLME modeling as part of clinical pharmacotherapy was first applied to pharmacokinetic analysis. Now the methodology is adapted to include analysis on almost any part of human (patho)physiology.

4.2 Nonlinear mixed effects modeling

4.2.1 Early applications

NLME modeling of pharmacokinetic data was first introduced by Lewis B. Sheiner, a clinician, and Stuart Beal, a statistician (100). In the 1970's they adapted the NLME modeling technique to utilize therapeutic drug monitoring (TDM) data for dose optimization of digoxin and warfarin therapy. Typical data from TDM comprised of 2-3 drug concentration measurements per patient, i.e. sparse data. Such data was not used in pharmacokinetic analyses as the methodology of that time required the use of "rich" concentration-time profiles where data often consisted of 3-5 times more observations per subject than number of parameters estimated (100). In their pivotal publication Sheiner and colleagues showed the benefit of sparse data analysis for dose optimization of digoxin (101). Use of sparse data made large pharmacokinetic studies feasible which laid the foundation to the field of population pharmacokinetics.

The statistical software developed for the digoxin model was later extended into the general modeling software, NONMEM (102). Today NONMEM still is the most widely used software for analysis of pharmacokinetic and pharmacodynamic data on a population level (103).

Despite the value of NLME modeling, even now modeling results are sometimes overlooked. Possibly it is the statistical complexity of the subject that hinders its penetration into traditional clinical pharmacology. However, it may not be necessary to fully understand all the mathematical aspects of parameter estimation algorithms to take advantage of the results of a NLME analysis. A rudimental understanding of various parts of a NLME model and the ability to interpret parameter estimates is often enough to appreciate and understand the results.

4.2.2 Components of a nonlinear mixed effect model

A NLME model can generally be divided into two components: the *fixed* and the *random effects,* Figure 5. The fixed effect consists of parameters describing the underlying structure of the system of interest, e.g. the components of a pharmacokinetic model for the typical individual. In its simplest form, a pharmacokinetic model of an intravenously administered drug is defined by Equation 1.

$$C_p = \frac{dose}{V} \cdot e^{\left(-\frac{CL}{V}t\right)} \qquad \text{Equation 1}$$

Where Cp is the predicted drug concentration measured in plasma at time, t, V is the volume of distribution and CL is the elimination clearance. The fixed effects parameters of this model are thus CL and V.

In NLME modeling the typical parameter estimates and between subject variability of those parameters are simultaneously estimated. The between subject variability of fixed effects parameters are part of the random effect model, Figure 5. The relationship between the individual estimates of a model and the estimate for the typical individual can be described by Equation 2.

$$V_i = V \cdot e^{\eta_i} \qquad \text{Equation 2}$$

where V_i is the individual estimate of the volume of distribution and V is the estimate for the typical individual in the population. The η is a random effect accounting for the individual difference from the typical estimate. The η estimates are normally distributed with the mean of zero and variance of ω^2.

While a quantification of between subject variability is an important part of the population approach the true strength of the method is when this variability can be explained by some measurable patient factor, a covariate. The relation between the individual parameter estimates and covariates such as sex, bodyweight or genetic polymorphism, are quantified in the covariate model, Figure 5.

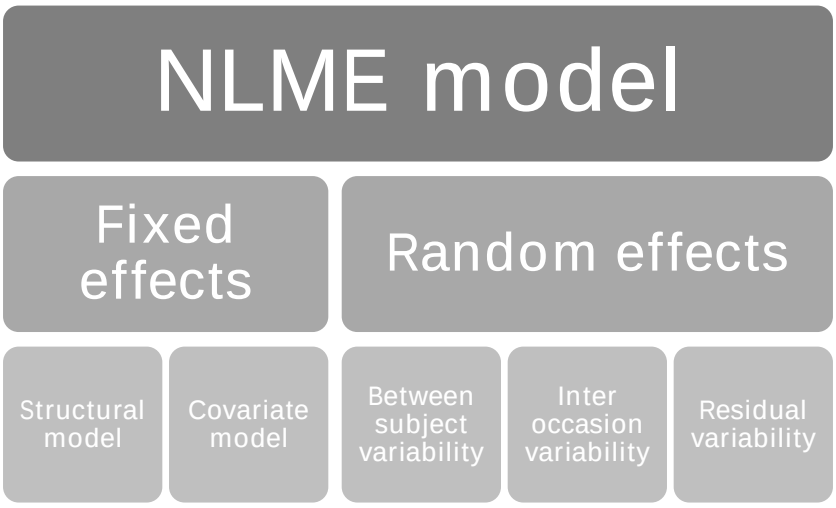

Figure 5. Components of a nonlinear mixed effect (NLME) model.

The difference between males and females in terms of volume of distribution is exemplified in Equation 3.

$$V_i = V \cdot (1 + \theta \times Sex) \times e^{\eta_i} \qquad \text{Equation 3}$$

In this example θ is the factorial change in the typical volume of distribution in females compared to males. Sex is a categorical identifier where e.g. males are coded as 0 and females as 1. By attributing some of the between subject variability of V to differences in sex one could reduce the estimate of the variance of V (ω^2) in Equation 2.

Variability in pharmacokinetics is known to vary with time. Sometimes the reason for the variability is known, e.g. change in weight, concomitant medications or progression of some disease. In such cases one alternative is to treat the known factors affecting variability as time-varying covariates (104). Other approaches are available when the variability is dependent on an unknown or unobserved covariate. One such approach is the addition of interoccasion variability (IOV), Figure 5. If subjects in the study have been observed multiple times per occasion and if there are two or more occasions then an IOV model may be justified. Failure to account for IOV can lead to biased parameter estimates and inflated residual variability (105).

The remaining variability, which is not explained by the random effects models or covariate models, is lumped into the residual error model, Figure 5. In the residual error one accounts for model misspecification, assay error, error in dosing history and sampling time. Many models that account for residual variability are possible. One approach is, nonetheless, more popular than others. A model consisting of an additive (ε_{add}) and a proportional (ε_{prop}) part, with mean of zero

and variance of σ^2, is specified in Equation 4. The residual model quantifies the remaining difference between the individual predictions (IPRED) and individual observations (Y). If either the proportional or the additive part of the model is estimated near zero, the model may be reduced to include just one variance component.

$$Y = \text{IPRED} + \text{IPRED} \cdot \varepsilon_{prop} + \varepsilon_{add} \quad \text{Equation 4}$$

4.3 Mechanistic viral dynamics models

NLME modeling, first applied to pharmacokinetics, has evolved to include more complex systems relevant to human (patho)physiology, such as the interplay between HIV-1 virus and CD4 cells.

Viral dynamics models are mathematical representations of the interaction between virus, the host cells and the effect drugs exhibit on the interaction. The original model describing this type of systems is based on the predator-prey concept introduced in epidemiology by Alfred J. Lotka and Vito Volterra. Lotka and Volterra introduced the concepts independently of each other roughly at the same time (106).

The interplay between the virus and the host's cells is represented by equations describing the populations of uninfected cells that have the potential to be infected (target cells [T]), the already infected cells (I) and the free virus particles (V), Equations 10, 11 and 13. Cells that are infected but do not produce virus (latently infected [L]) have the potential to become actively infected, Equation 12. Virus is produced by actively infected cells with the rate of p. Virus can be eliminated from body by rate of c or infect uninfected cells with infection rate of *i*. Uninfected cells are born (*b*), eliminated by natural death rate (d_1) or transformed to latently or actively infected cells. The fraction transformed to actively infected cells is determined by *Fr*. Actively infected cells are eliminated with death rate of (d_2). Latently infected cells can be transformed into actively infected by activation rate *a* or eliminated by death rate d_3. Drugs can act by inhibiting infection or production of infectious virus. In Equations 5 to 8 the inhibitory effect on infection is represented by INH which can range from 0 (no inhibition) to 1 (maximum inhibition).

$$\frac{dT}{dt} = b - d_1 \times T - (1 - INH) \times i \times V \times T \quad \text{Equation 5}$$

$$\frac{dA}{dt} = Fr \times (1 - INH) \times i \times V \times T - d_2 \times A + a \times L \quad \text{Equation 6}$$

$$\frac{dL}{dt} = (1 - Fr) \times (1 - INH) \times i \times V \times T - d_3 \times L - a \times L \quad \text{Equation 7}$$

$$\frac{dV}{dt} = p \times A - c \times V \qquad \text{Equation 8}$$

Various versions of this model have been applied to monotherapy studies (107,108) as well as large multicenter trials with standard HAART therapy (109). In the latter case the INH level was estimated separately for each regiment tested (atazanavir/r, efavirenz, lopinavir/r) while in the former case the INH was drug concentration dependent.

4.4 The bottom up approach – *in vitro in vivo* extrapolation

The focus in *in vitro-in vivo* extrapolation (IVIVE) lies in prediction of human pharmacokinetics and its variability in different populations using *in vitro* data. This methodology can be of great use in drug development where it can narrow the bridge between preclinical and clinical drug development. Its applications may also save considerable time and resources by investigating the potential for drug-drug interactions in virtual populations using *in silico* trials.

IVIVE utilizes the increased understanding of pharmacokinetics and by which mechanism covariates such as pharmacogenetics, sex, age, body weight, concurrent medication, renal impairment *etc.*, can influence drug exposure in man to *a priori* estimate the effects of covariates in study populations (110,111).

This approach relies on *in vitro* methods to estimate parameters such as logP, *in vitro* intrinsic CL, plasma protein binding and others. These parameters are then extrapolated to *in vivo* on a population level. The IVIVE method is for this reason referred to as "the bottom up approach" as opposed to NLME modeling which in some cases can be referred to as the "top down approach".

4.4.1 Components of the *in vitro - in vivo* extrapolation model

The IVIVE model can be described as a union of three (sometimes four) components (110–112).

1) The structural model. A physiologically based pharmacokinetic model describing the various tissues in man connected by the circulatory system.
2) The system specific parameters. Parameters describing human physiology relevant to pharmacokinetics which are independent of the studied drug.
3) The drug specific parameters. Parameters specific to the investigated drug.

Parameters describing the execution and simulation of a particular study design are sometimes referred to as a forth component of the IVIVE model (112). A recent review of physiologically based pharmacokinetic modeling by Rowland *et al.* can provide interested readers with extensive information about the first component of the IVIVE model (112). Here, the main focus lies in distinction between the drug and the system specific parameters and their effect on pharmacokinetic variability. Hepatic clearance (CL_H), will serve as an example due to its complexity and its importance to drug exposure in man.

Assuming the well-stirred model (113), unbound drug enters the hepatocytes through a passive process determined by the hepatic blood perfusion and is thus available for metabolism. The determinants of CL_H are thus the fraction of the drug unbound in blood (fu), unbound intrinsic metabolic clearance (CLu_{int}) and hepatic blood flow (Q_H), Equation 9.

$$CL_H = \frac{Q_H \times CLu_{int} \times fu}{Q_H + CLu_{int} \times fu} \qquad \text{Equation 9}$$

Variability in hepatic blood flow, which is a function of cardiac output, is greatly explained by interindividual differences in body size and age (110). Additionally, external factors such as food intake, posture and physical activity are known to add to intra- and interindividual variability of cardiac output (110). Unless pharmacologically affected by the investigated drug, Q_H is a pure system specific parameter. If the product of fu and CLu_{int} is much larger than Q_H i.e. extraction ratio (E_H)[2] is over 0.7, CL_H can be approximated to liver blood flow (114), Equation 10. In such cases the limiting factor to the hepatic elimination is hepatic blood flow rendering hepatic clearance relatively insensitive to changes in plasma protein binding or induction/inhibition of hepatic eliminating enzymes. Morphine, verapamil and cocaine are drugs known to be administered intravenously with a high extraction rate and mainly eliminated by hepatic metabolism (115).

When $E_H > 0.7$ $\qquad CL_H \approx Q_H$ $\qquad$ Equation 10

The fraction of drug bound in blood is determined by both system and drug specific parameters (110). System parameters include the amount of circulating erythrocytes and various plasma proteins while the drug's affinity to proteins and erythrocytes is a drug specific parameter dependent on the physiochemical properties of the compound (110,111). Affinity to plasma protein can be measured or predicted *in silico* (116). Variation in hematocrit and plasma proteins due to sex, age, disease etc. can be accounted for in the IVIVE model. Recently, Ohtani *et al.* showed the influence of hematocrit on the clearance of tacrolimus using an IVIVE model (117).

[2] Extraction ratio is defined as the ratio of the rate of elimination to the rate of presentation (114).

Unbound intrinsic clearance is a measure of the total hepatic capacity to metabolize the drug of interest. For low extraction drugs (E_H<0.3) i.e. when Q_H is larger than the product of f_u and CLu_{int}, Equation 9 can be reduced to Equation 11.

When E_H <0.3 $$CL_H \approx \mathrm{CLu_{int}} \times \mathrm{fu}$$ Equation 11

Diazepam and warfarin are drug exhibiting a low extraction rate, known to be administered intravenously and are mainly eliminated through hepatic metabolism (115). It is nevertheless important to clarify that oral elimination clearance (CL_{po}) is dependent on intrinsic clearance and fraction unbound in blood irrespective of low or high extraction rate, Equation 12.

When E_H 0.3< or >0.7 and CL≈CL_H, F_{abs}=1 $$CL_{po} \approx \mathrm{CLu_{int}} \times \mathrm{fu}$$ Equation 12

4.4.2 Prediction of intrinsic hepatic clearance

Intrinsic hepatic clearance is perhaps the most complex and pivotal parameter that needs to be accounted for if one wishes to predict pharmacokinetic properties of a drug by the use of an IVIVE model. Intrinsic hepatic clearance can be expressed as the ratio of the maximum metabolizing rate (V_{max}) and the Michaelis Menten constant (K_m) of all metabolizing enzymes when concentration of drug is lower than K_m (110). Under such conditions, V_{max} and K_m can be experimentally determined by use of liver microsomes, hepatocytes or recombinantly (rh) expressed enzymes (110,118). Using recombinantly expressed enzymes, experimentally determined intrinsic clearance for a system can be extrapolated to total liver intrinsic clearance by Equation 13 (110,119).

$$CL_{int} = \left[\sum_{j=i}^{n}\left(\sum_{j=i}^{n} ISEF_{ji} \times \frac{V_{\max i}(rhCYP_{\ i}) \times CYP_j abundance}{K_{m\,i}(rhCYP_j)}\right)\right] \times MPPGL \times LW$$

Equation 13

where j is the CYP isoform; i is the metabolic pathway, MPPGL is the amount of microsomal protein per gram of liver, CYP_j abundance is the amount (pmol) of the j isoform per mg of microsomal protein, LW is liver weight and ISEF stands for inter system extrapolation factor. ISEFs are factors that correct for the difference in activity per unit enzyme between recombinant and native human enzyme (118).

In the case where V_{max} and K_m are determined, the only true drug specific parameter seems to be K_m, which is inversely proportional to the affinity of the drug to the metabolizing enzyme. Other parameters in the equation are system specific. In the case of ISEF, the parameter is specific to an *in vitro* system while CYP_j abundance, MPPGL and LW are specific to human physiology.

4.4.3 Prediction of variability in intrinsic hepatic clearance

Perhaps equally important to predicting intrinsic CL in man is the prediction of the variability as well as its determinants. Equation 13 allows for introduction of physiological meaningful variability through several of its parameters.

The relationships of determinants and the variability of parameters can sometimes be complex. Age is an influential determinant or covariate for variability in CYP abundance as well as MPPGL and LW (111). MPPGL increases from birth to a peak value of 40 mg/g at age 28. At age 65 this value has decreased by approximately 25% to 29 mg/g (120). When examining all non-adult populations, age is the main determinant for body weight and height which provides a relation to liver weight through body surface area (BSA) (121). Liver weight is related to BSA by the following equation, $LW=0722 \cdot BSA^{1.176}$. Japanese subjects are found to deviate from Caucasians by having 19% larger livers for a given bodyweight (121).

CYP abundance can, beside age, incorporate variability due to genetic polymorphism, ethnicity, sex and external inducers. Females have been shown to have significantly higher CYP3A4 abundance compared to males, 113 vs 75 pmol/mg (122).

Polycyclic aromatic hydrocarbons in cigarette smoke are known inducers of CYP1A2 through the aryl hydrocarbon receptor/Ah receptor nuclear translocator (AhR/Arnt) (123). The relation between the number of cigarettes smoked and the hepatic CYP1A2 abundance was recently quantified. Heavy smokers (>20 cigarettes per day) where estimated to have a 1.8 fold increase in CYP1A2 abundance relative to non-smokers (124). In this particular publication, the authors used a NLME model to quantify the relationship between smoking and caffeine clearance in order to estimate the influence of smoking on CYP1A2 abundance. Since both the bottom up and the top down techniques were used, this method is referred to as the middle out approach.

Ethnicity is a significant factor for explaining variable distributions of genetic polymorphisms in man. For example, the frequency of the CYP2B6*6 allele is highly variable with ethnicity in some African population up to 45.5% while its spread in European and Asian populations is substantially lower, 21.4 and 17.4%, respectively (42,43).

In conclusion, knowledge of fundamental pharmacokinetics as well as human physiology can be used to predict not only the typical population estimates of pharmacokinetic parameters but also their variability due to genetic, physiological, and demographic variables. Combining the top down to the bottom up approach can allow creation of more mechanistic models that not only describe a single study but also predict variability in a larger population.

4.5 IVIVE versus NLMEM

IVIVE should not be seen as an alternative to nonlinear mixed effects modeling but rather as its compliment. The versatility of NLME modeling has led to its application to all stages of drug development, from first-time-in-man studies to post marketing phase IV trials. NLME modeling allows pharmacokinetics to be linked with pharmacodynamics of biomarkers as well as hard endpoints. Models can be used to simulate clinical trials sometimes to support clinically untested doses (125). Additionally, modeling can lead to increased understanding of the disease separating the target population from non-responsive patient subpopulations (98). In contrast to IVIVE where current focus is on pharmacokinetics, NLME modeling can be seamlessly adapted to complex systems ranging from highly mechanistic platform models such at the glucose-insulin model for type II diabetes (126) to complex but empirical Markov models of drugs effect on sleep stages (127).

4.6 Model based design and analysis of phase II HIV-1 trials

4.6.1 Framework of phase II trials in antiretroviral drug development

Phase IIa trials serve to show the clinical efficacy of drug candidates in clinical development i.e. proof of concept (POC). Additionally, these trials help to identify the dose to be tested in Phase IIb (107). Whereas Phase IIb HIV-1 trials can be relatively large (70-80 patients/arm) and long (24-48 weeks) phase IIa trial are small (8-11 subject/arm) and short (10 days of therapy) (128–132). In phase IIa, the drug candidate is administered without concomitant backbone therapy (128–132). The risks of resistance development in monotherapy are justified by the need to quantify the relation between dose/concentration and antiretroviral response (133). Monotherapy trials are nevertheless recommended to be as short as possible (133). To discriminate between several active doses and to aid in dose selection for phase IIb trials, European Medicines Agency (EMA) recommends comparison against active control (133).

The typical mean study endpoint is the mean change HIV-RNA levels from baseline and a single time point, usually at the end of treatment or at nadir. Despite the relative homogeneity in the study designs of phase IIa trials, there appears to be no consensus on which statistical test is most appropriate to test POC, Table 1.

Table 1. Characteristics of recent phase IIa HIV-1 trials

Reference	Primary endpoint	Statistic used	Number of arms	Placebo
(132)	Mean change in HIV-RNA (log10) at day 11	Williams step-down test	10 (8-9 patients/arm)	2 placebo arms [a] (4 and 12 patients/arm)
(131)	Mean change in HIV-RNA (log10) at day 8	Mann–Whitney U	5 (n=9)	1 (n=11)
(128)	Mean change in HIV-RNA (log10) at day 8	Model based	8 (n=6)	1 (n=6)
(129)	Mean change in HIV-RNA (log10) at day 9	ANCOVA and t-test	5 (n=9)	1 (n=12)

[a] pooled placebo arms from two studies

4.7 Power of clinical trials

The cost of clinical trials is approximately proportional to enrolled number of subjects, excluding some fixed costs (134). Determining the required number of subjects is based on the power to detect a clinically relevant and statistically significant improvement in the treated compared to the placebo group. This improvement is often set to a mean difference corresponding to a p-value below 0.05. Besides method of analysis, statistical power is influenced by the type I error, standard deviation of the variable and the sample size. Increasing type I error would result in an increased power but also an increased risk of falsely rejecting the null hypothesis, i.e. the drug is thought to have an effect when no effect is present. Reducing the standard deviation of the samples is sometimes possible with stringent inclusion criteria for trials; this approach is often indirectly applied in early phases of drug development. Possible consequence of this approach is loss of gained knowledge about interindividual variability in early drug development due to too homogenous patient populations. And, finally, increasing the sample size is possibly the most costly method to increase the power of the study. The choice of statistical method to analyze the effect size poses therefore an opportunity to influence study power with minimal effect on cost and knowledge gained.

Applying the model based approach to analyze clinical trials has been demonstrated to increase the power to detect true differences. The utility lies in the ability to use longitudinal analysis, combining all observations from all subjects and dose levels in a simultaneous analysis and also including missing data due to dropout (135). A statistical method that increases the power of the study can reduce cost as well as unnecessary exposure to untested new treatments (134).

4.8 Model based hypothesis testing and power calculation

4.8.1 Stochastic simulations and re-estimations

The objective function value (OFV) is a global measure of goodness-of-fit of a model and is proportional to -2 times the log of the likelihood of the data. Pharmacometric or model based hypothesis testing can be based on the log likelihood ratio (LR) test of the difference in OFV between two nested models. The full model assumes an existing drug effect [H_1], while the reduced model assumes no drug effect [H_0], where H_0 and H_1 correspond to the null (no difference between groups: $\mu_1 = \mu_2$) and the alternative hypothesis (difference between groups: $\mu_1 \neq \mu_2$), respectively. The difference in objective function (ΔOFV), or log-likelihood ratio, is assumed to follow the χ^2 distribution. The null hypothesis can be rejected if the drop in OFV exceeds a predetermined significance level (often 0.05) for the corresponding difference in degrees of freedom (Δ*df*). The Δ*df* is determined by the difference of estimated number of parameter in the full and the reduced model.

Stochastic simulation and re-estimation (SSE) can hence be used for calculation of statistical power. A large number of trials e.g. one thousand are simulated with the full model, in which assumptions about the drug effect and its variability are made. Both the reduced and the full model are fitted to the simulated trials. Power is calculated as the proportion of trials where the full model has significantly lower OFV compared to the reduced model (n), Equation 14. The procedure is repeated for every sample size one wishes to calculate power for.

$$Power = \frac{\sum_{n=1}^{N}\left(\Delta OFV \geq \chi^2{}_{0.05}(df)\right)_n}{N} \qquad \text{Equation 14}$$

SSE can be a time-consuming endeavor for large models, sometimes spanning over several months. Further, a correction for type I error inflation has to be made in cases where the sample size is small (136,137).

4.8.2 Monte-Carlo Mapped Power

With the introduction of Monte-Carlo Mapped Power method by Vong *et al.*, the speed of power calculations has significantly increased (138). Instead of simulating and re-estimating a large number of datasets, a single very large study is simulated (with the full model) and re-estimated (with the full and the reduced model). The sum of individual OFVs (iOFV) is equal to the total OFV (Equation 15). The difference between iOFVs of the full and the reduced model is equivalent to total ΔOFV, Equation 16.

$$OFV = \sum_{j=1}^{n} iOFV_j \qquad \text{Equation 15}$$

$$\Delta OFV = \sum_{j=1}^{n} iOFV_{j_{FULL}} - \sum_{j=1}^{n} iOFV_{j_{REDUCED}} \qquad \text{Equation 16}$$

Individual ΔOFVs are computed from the two estimations and resampled 10 000 times for each sample size. The fraction of the 10 000 samples where the iΔOFV is greater than the threshold level, defined by the number of *df* and significance level, is the power for that sample size.

In addition to improvement in speed, adjustment for type I error is no longer needed (138). Previously, the MCMP method has successfully been applied to a number of pharmacokinetic and pharmacodynamic examples (138,139).

5 AIMS OF THE THESIS

The overall aim of this thesis was 1) to improve the treatment of the HIV-1 infection by optimization and individualization of antiretroviral pharmacotherapy and 2) to shown the benefits of pharmacometrics, as part of model based drug development, for the design, analysis and interpretations of clinical trials and their outcomes. This is exemplified by quantitative analyses of efavirenz and atazanavir treatments as well as simulations of phase II HIV-1 trials. The five papers in this thesis aim to answer the following questions.

1. Can an *in vitro-in vivo* extrapolation model be used to assess the current recommendations when efavirenz is co-administered with rifampicin? (Paper I)

2. What is the influence of the HIV-1 infection of the pharmacokinetics of efavirenz? (Paper II)

3. What is the quantitative relationship between atazanavir plasma concentrations and bilirubin elevations in patients? (Paper III)

4. Is bilirubin a good tool for assessing atazanavir exposure and adherence in HIV-1 infected patients? (Paper IV)

5. What are the benefits of a model based drug development approach in terms of sample size, analysis and interpretation of results in Phase II HIV-1 trials? (Paper V)

6 PATIENTS AND METHODS

6.1 Paper I – Efavirenz and rifampicin

6.1.1 In *Vitro - In vivo* extrapolation

The general methodology of *in vitro-in vivo* extrapolation has been described in the introduction of this thesis (section 4.4). The physiologically based simulator, Simcyp version 8.2 (140) (Simcyp™ Ltd, Sheffield, UK), was used for IVIVE of efavirenz and rifampicin pharmacokinetics and simulation of their interaction.

Parameters needed for the efavirenz IVIVE model were found in literature, obtained through *in silico* prediction or estimated using data provided in the literature (Table 2). Parameters associated with rifampicin pharmacokinetics and induction properties were largely provided by the software with the exception of rifampicin's influence on CYP2B6 which were estimated from Faucette *et al.* (141). When parameter estimates were not directly provided by the literature the experimental data was obtained from tables or digitalized from graphs by graph digitalizing software. Obtained data was subsequently modeled using WinNonlin vesion 5.2 (Pharsight Co., Mountain View, CA, USA).

The efavirenz volume of distribution (3.33 L/kg) was scaled from rat to man by allometric scaling and together with LogP used as input for prediction of tissue partitioning constants (K_p), as proposed by Jansson *et al* (142). The predicted K_p values for the various tissues were as follow: lung: 63.3, heart: 5.25, kidney: 3.87, brain: 4.57, spleen: 0.67, gut: 1.54, liver: 3.70, bone: 0.54, muscle: 0.67, skin: 0.85 and fat: 12.6.

6.1.2 Model validation

Before any prediction in regards to the interaction between efavirenz and rifampicin could be done, the efavirenz model was validated against data from three clinical studies. The first study was a single dose study in 121 Ugandan healthy volunteers. The other two studies were conducted in patients in Zimbabwe (n=74) and Sweden/Norway (n=76) at steady-state (38,39,94). Ethical approval for the Ugandan study was given by the Uganda National Council of Science and Technology. The second study from Zimbabwe was approved by ethics committees at the Medical Research Council of Zimbabwe and by the Joint Parirenyatwa Hospital and College of Health Science Research, Harare. The third study was approved by an independent ethics committee and the Swedish Medical Products Agency.

Simulations were performed where the three studies were emulated in terms of age, sex and frequency of slow metabolizers. The resulting plasma concentra-

tion-time curves were visually compared. Derived pharmacokinetic parameters (C_{max}, T_{max}, CL/F and AUC) of the single dose study were compared to those of the corresponding simulation study.

The level of efavirenz autoinduction was evaluated by comparison to clinical estimates of efavirenz CL/F at steady state. The extent of rifampicin influence on efavirenz CL/F was likewise compared to clinical estimates.

6.1.3 Simulation of interaction

Once validated, the model was used to simulate an efavirenz dose adjustment from 600 to 800 mg in a population of 400 virtual patients. The 400 patients were stratified based on CYP2B6 phenotype (slow vs. extensive metabolizer) and body weight (below or above 50 kg). Each stratum consisted of 100 patients. Two scenarios were simulated in each stratum: 600 mg of efavirenz with and without rifampicin and 800 mg efavirenz with and without rifampicin. Slow and extensive metabolizers were predefined in the Simcyp software by CYP2B6 abundance levels (SM=6, EM=17 pmol·(mg protein) $^{-1}$, respectively. The magnitude of the interaction was evaluated based on CL/F, C_{max}, C_{trough} and AUC at steady state.

Table 2. Simcyp input parameters

Efavirenz input parameters	Value	Variability (CV%)	Comments and references
MW	315.67		(22)
LogP	5.4		(143)
B:P ratio	0.74		(144)
Plasma fu	0.0112		Predicted by Simcyp
Caco-2 permeability (10^{-6} cm/s)	8.92		(145)
fu (Gut)	1		Assumed
Main binding protein	Albumin		(22)
fu(mic)	0.3		Predicted (146)
fu(hep)	0.063		(147)
rCYP 3A4 V_{max} (pmol/min/pmol 3A4)	0.16		Baculovirus ISEF (31)
rCYP 3A4 K_m (μM)	23.5		Baculovirus ISEF (31)
rCYP 3A5 V_{max} (pmol/min/pmol 3A5)	0.6		Baculovirus ISEF (31)
rCYP 3A5 K_m (μM)	19.1		Baculovirus ISEF (31)
rCYP 1A2 V_{max} (pmol/min/pmol 1A2)	0.6		Baculovirus ISEF (31)
rCYP 1A2 K_m (μM)	8.3		Baculovirus ISEF (31)
rCYP 2B6 V_{max} (pmol/min/pmol 2B6)	3.5		Baculovirus ISEF (31)
rCYP 2B6 K_m (μM)	6.4		Baculovirus ISEF (31)
rCYP 2A6 V_{max} (pmol/min/pmol 2A6)	1.08		Converted from Vmax(HLM) (32) as proposed by (118)
rCYP 2A6 K_m (μM)	14.7		(32)
UGT2B7 V_{max} (pmol/min/mg)	1.5		(148)
UGT2B7 K_m (μM)	16.1		(148)
CYP 3A4 Indmax	6.45	18.6	Digitalized data (147) modeled together with (35)
CYP3A4 IndC50 (μM)	3.93	52.5	Digitalized data (147) modeled together with (35)
CYP 2B6 Indmax	5.76	13.7	Modeled from (34)
CYP 2B6 IndC50 (μM)	0.82	71.9	Modeled from (34)
Rifampicin input parameters	**Value**	**Variability[a] (CV%)**	**Comments and references**
CYP2B6 Indmax	8.5[b]	30	(141)
CYP2B6 IndC50 (μM)	1.17	30	(141)
fu (hep)	0.419		(147)

[a] Default Simcyp setting,Indmax Maximal fold induction over vehicle (1 = no induction).[b] mean value (n=2), V_{max} Maximum rate of metabolism, fu(mic) fraction unbound in microsomes, Km Michaelis-Menten constant, ISEF Inter System Extrapolation Factor, plasma fu unbpund fraction in plasma, B:P ratio Blood:Plasma concentration ratio, MW molecular wheight, Log P logaritm of octanol:water ratio

6.2 Paper II – Efavirenz pharmacokinetics and HIV/AIDS

6.2.1 Study design

The objective of this study was to investigate potential differences in the pharmacokinetics of efavirenz in healthy volunteers versus HIV-1 patients. Efavirenz plasma concentration in 29 treatment naïve HIV-1 patients was measured predose and 1, 2, 3, 4, 6, 8, 16 and 24 hours after the first dose of 600 mg. All patients received zidovudine/lamivudine (150/300 mg) as backbone therapy. Additionally, all patients were administered cotrimoxazole (trimethoprim /sulfamethoxazole) during the study period. Included patients were eligible for ARV treatment, based on CD4+ cell count.

Data from the HIV-1 patients was merged with data from a previously published pharmacokinetic study on efavirenz pharmacokinetics in healthy volunteers (38). Plasma from 32 healthy volunteers was collected and efavirenz concentrations quantified at 0, 1, 2, 4, 8, 24, 48 and 72 hours after a single dose of efavirenz (600 mg). Potential pharmacogenetics, demographic and biochemical covariates were specified *a priori*.

Ethical approvals were obtained from the Uganda National Council of Science and Technology (Kampala, Uganda) and Karolinska Institutet (Stockholm, Sweden). All participants gave written informed consent.

6.2.2 Model development

A two-compartment model with sequential zero- to first order absorption previously used to describe efavirenz pharmacokinetics in healthy volunteers was used as a starting point (38). Clearance and volume of distribution parameters where allometrically scaled for body weight (BW) and centered to the median BW. The scaling factor was fixed to ¾ and 1 for clearance parameters and volumes, respectively (149).

Models with 1 or 3 compartments were used to challenge the initial 2-compartment model. A variety of absorption models were tested, including a transit compartment absorption model (150). Between-subject variability was initially tested for all pharmacokinetic parameters but only kept if they were estimated with reasonable precision and resulted in reduction of the objective function value.

The stepwise covariate model building tool implemented in the PsN package (151) was used for forward covariate selection and backward deletion in an automated fashion. Inclusion criteria for the forward step was a reduction in OFV corresponding to a p-value of ≤ 0.05 while the backward deletion criteria was more stringent where covariates were only kept if their deletion resulted in an OFV increased corresponding to a p-value of ≤ 0.01. Final covariate relationships

had to reduce the estimated between subject variability. The 95% confidence interval of the final covariate was required not to include zero for continuous and one for categorical covariates.

6.2.3 Data analysis

The general methodology of NLME modeling has been described in section 4.2.

Modeling software NONMEM, version VI (Icon Development Solutions, Ellicott City, MD, USA) was used to fit nonlinear mixed effects models (152). The first-order conditional estimation method with interaction was used (FOCE-I). Models were discriminated using the OFV criteria, precision of parameter estimates and goodness of fit plots. Auxiliary software e.g. Census 1.1 (153), Xpose 4.0 (154), PsN (151) and Spotfire software (Tibico Software, Somerville, MA, USA) was used for data evaluation, graphics, handling of output files, model evaluation and covariate modeling.

6.3 Paper III - Atazanavir and bilirubin

6.3.1 Study design

The present work included the atazanavir/ritonavir arm of the previously published NORTHIV study (93,94,109). In brief, the NORTHIV study was a randomized, multicenter, open-label trial with three arms (efavirenz, lopinavir/ritonavir and atazanavir/ritonavir) conducted in Sweden and Norway. The atazanavir/ritonavir arm consisted of 82 treatment naïve patients. The backbone therapy was allowed to vary according to clinical practice. In addition to patients' demographics, this analysis included atazanavir plasma concentrations and bilirubin observations up to three years after study enrolment at 5 occasions (weeks: 4, 12, 48, 96 and 144 after enrollment). In total, 361 bilirubin concentrations and 200 atazanavir steady state plasma samples were available.

The NORTHIV study protocol was approved by the Research Ethics Committee of the University of Gothenburg, the Regional Committees for Medical Research Ethics in Norway and the Swedish Medical Products Agency. All patients provided a signed informed consent prior to enrolment.

6.3.2 Model development

A previously developed and validated model for atazanavir/ritonavir pharmacokinetics was used as an initial starting point (75). The atazanavir plasma concentrations were transformed into their natural logarithms. Due to limited number of plasma samples in the absorption phase, the lag-time and the first order absorption rate constant had to be fixed to literature values (75). Estimated pharmacokinetic parameters were scaled by patients' bodyweights and centered to the population median bodyweight (70kg). The scaling factor was *a priori* fixed to 1

for volumes and at ¾ for clearance (149). Between-subject variability of parameter estimates was initially estimated for all pharmacokinetic parameters, but only kept if estimated with adequate precision and resulted in a significant drop in objective function value. Correlation between variably of fixed structural parameters was evaluated.

The final pharmacokinetic model was fixed and allowed to drive the bilirubin response in the pharmacodynamic models tested. Individual atazanavir observations were kept in the dataset. The concentration dependent inhibition of bilirubin conjugation was explored with multiple pharmacodynamic models, including the direct effect model, bio-phase distribution model and various indirect response models. Estimates of (uninhibited) bilirubin half-life from the final PKPD model were compared to estimates found in literature (155).

6.3.3 Simulations with the final model (Deterministic)

The final PKPD model was implemented into the Berkeley Madonna software (156). Three non-adherence scenarios were simulated where the typical patient misses one, two or three atazanavir doses.

Further, the pharmacokinetic model was fixed to result in atazanavir trough concentrations at the minimum effective concentration (MEC) of 0.2 µmol/L. The influence of baseline bilirubin concentrations (ranging from the lowest to the highest observed) on the trough concentrations of bilirubin at steady state was simulated. The various baseline values and their corresponding trough bilirubin concentrations at steady state were used to construct the atazanavir-bilirubin nomogram with the intention to be of use for detection of suboptimal exposure or non-adherence.

6.3.4 Data analysis

Procedures and the software used were identical to those used in paper II as described by section 7.2.3 Data analysis, with addition of Piraña as NONMEM project managing software (157) and Berkeley Madonna (156) used for simulation.

6.4 Paper IV – Validation of the atazanavir nomogram

6.4.1 Study design

The external validation dataset consisted of patients from Italy, Norway and France. The Italian patients were part of the therapeutic drug monitoring programs at the University of Torino. Both ritonavir boosted (n=56) and unboosted (n=56) patients were included but analyzed separately. All patients were on a 300/100 mg QD atazanavir/ritonavir regimen except two who were on a 200 and 400 mg QD based regimen, respectively. The unboosted patients' regimen varied from 200 mg BID to 400 mg QD. The backbone therapy was allowed to vary according to clinical practice. The bilirubin steady state samples were collected on average at 09:23 (±1:05) am, while baseline samples were collected between 8:00 and 11:00 am. Approximately 23% of the Italian cohort was coinfected with hepatitis B/C.

The data for the Norwegian patients was extracted from the Thematic Biobank "Infectious Diseases". All patients (n=76) were part of the HIV monitoring program at Oslo University Hospital where they were allocated to an atazanavir/ritonavir (300/100 mg QD) containing regimen. The backbone therapy varied according to clinical practice. The average times for bilirubin baseline and steady state sampling was 10:13 am (±1:38) and 09:44 (±1:22) am, respectively.

The French patients were part of the ANRS 134 -COPHAR 3 study (158). Of the 35 patient recruited to the study, one was excluded from this analysis due to a missing bilirubin baseline measurement. The patients were administered atazanavir/ritonavir (300/100 mg QD) and tenofovir/emtricitabine (245/200 mg) for 24 weeks. Matching bilirubin and atazanavir observations were available at weeks 4, 8, 16, and 24. On average the samples were collected 18.27 hours after dose. Hepatitis B/C was an exclusion criterion of the trial.

6.4.2 Application of the nomogram

The nomogram was applied to the bilirubin observations of the patients. Patients who were identified by the nomogram to have suboptimal atazanavir exposure were labeled as positive. If the prediction was correct or incorrect they were identified as true positive (TP) or false positive (FP), respectively. True negative (TN) and false negative (FN) observations were labeled and identified in the same manner. The nomogram's predictive properties were described in terms of specificity, sensitivity, accuracy, negative predictive value and positive predictive value, as defined in Table 3.

Table 3. Equations and interpretations of the metrics used to describe the predictive properties of the nomogram.

Equation	Interpretation
$Specificity = \frac{TN}{TN+FP}$	Specificity of the nomogram is the probability of a true negative result when the atazanavir sample is over MEC.
$Sensitivity = \frac{TP}{TP+FN}$	Sensitivity of the nomogram is the probability of a true positive result when the atazanavir sample is under MEC
$Accuracy = \frac{TP+TN}{TP+TN+FP+FN}$	Accuracy is the proportion of all correctly predicted observations for the nomogram.
$Negative\ predictive\ value = \frac{TN}{TN+FN}$	NPV is the probability of a negative test to be true negative
$Positive\ predictive\ value = \frac{TP}{TP+FP}$	PPV is the probability of a positive test to be true positive

MEC: minimum effective concentration (0.2 µmol/L), TP: true positive, TN: true negative, FP: false positive, FN: false negative, NPV: negative predictive value, PPV: positive predictive value

6.4.3 Simulation of non-adherence (Stochastic)

Stochastic simulations were used to determine if the nomogram could be used to detect periods of non-adherence in patients. The main difference from previous simulations based on this model is the introduction of random components (inter individual variability and residual error). Similar to the previous simulations: three scenarios (Scenarios 1-3) of non-adherence were evaluated. In Scenarios 1 to 3, 10% of the simulated patients (n=1000) were non-adherent for one, two or three consecutive days. In each of the simulated scenarios the patient were sampled at three sampling events (Event 1a, 1b and 2). Event 1a was at 24 hours after the period of non-adherence; Event 2 was 48 hours after the period of non-adherence; Event 1b was 25 hours after the period of non-adherence just after a patient self-administers an atazanavir dose without informing the clinical staff. The purpose of Event 2b is to conceal the non-adherence period by being adherent just before a sampling event. The scenarios and events are illustrated in Figure 6.

The nomogram identified a patient as non-adherent if the bilirubin concentration indicated an atazanavir exposure below MEC. Simulated atazanavir concentrations were used in a similar manner to identify the non-adherent patients. The two methods were evaluated based on the metrics in Table 3. All simulations were performed in NONMEM 7.12 (152) (ICON Development Solutions, Ellicot City, MD, USA) with the aid of PsN (151,159).

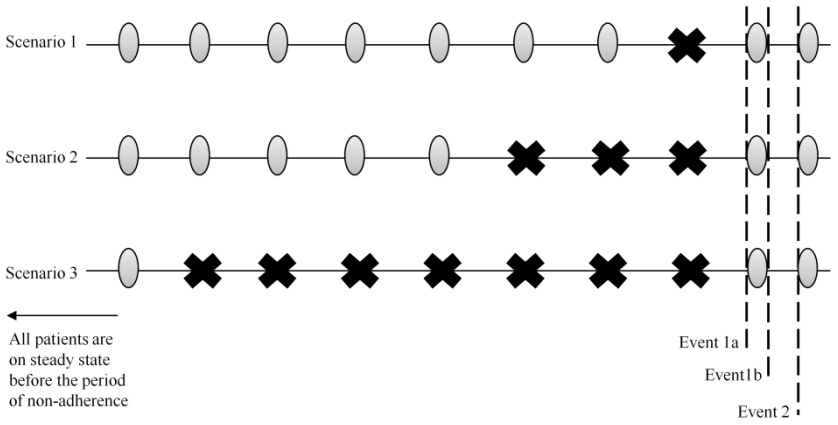

Figure 6. Study design for the simulation based validation. The crosses represent days of non-adherence to atazanavir while the ellipsoids represent administered doses. The dashed lines represent sampling/monitoring events. Event 1a: patients are monitored/sampled 24 hours after a period of non-adherence. Event 1b: patients are monitored/sampled 1 hour after an atazanavir dose event following a period of non-adherence. Event 2: patients are monitored/sampled 48 hours after a period of non-adherence.

6.5 Paper V – Phase II HIV-1 trials

6.5.1 HIV-1 dynamics model

A previously developed model of HIV-1 dynamics was used for all the simulations in this work (107,108). The model was briefly introduced in Section 4.3. When simulated, estimates of the viral parameters and their variability were fixed according to previously reported values (108,109).

6.5.2 Simulation of dose-finding/POC study

The dose-finding/POC study was assumed to consist of 4 dose arms and 1 placebo arm. Based on literature, Table 1, a typical Phase IIa trial was simulated where the patients were treated for 10 days and followed up to 40 days after treatment initiation. The drug effect was dose dependent and assumed to inhibit the infection of CD4+ cells (Equation 17). The maximum level of infection inhibition (INH) was assumed to be 1. The dose resulting in 50% of maximum inhibition (ED_{50}) was arbitrary set to 4 units. The tested doses (0.5, 2, 8 and 20) resulted in INH levels of 0.11, 0.33, 0.67 and 0.83, respectively. The viral load was simulated daily up to day 13 and thereafter at days 15, 19, 22, 25 and 40 (132).

$$INH = \frac{Dose}{ED50 + Dose}$$ Equation 17

The power to establish POC was calculated for various sample sizes based on t-test, ANOVA and the MCMP method. The null hypothesis [H_0] for the t-test was: the highest or the lowest tested dose results in the same mean viral load at day 10 as the placebo arm while [H_0] for ANOVA assumed same mean viral load at day 10 for all arms including placebo. The null hypothesis [H_0] for the MCMP method was: There is no significant dose response relationship (INH=0). The MCMP method has been described in detail in section 4.8.2.

6.5.3 Simulation of a comparison of investigational drug and active competitor

The settings of a phase II trial were used to identify the smallest difference in treatment effect possible to detect applying the HIV-1 dynamics model. The study sampling schedule was identical to the one of the dose-finding/POC trial. An Investigational drug (I.D.), with INH set to 0.61 resulting in a decrease in viral load of 1.32 $\log_{10}$ copies/mL at day 10 of monotherapy, was compared against a hypothetical competitor in four scenarios where the competitor varied in efficacy. The competitor (C), with INH set to 0.67, 0.74, 0.83 and 0.92, resulted in in 5, 10, 15, and 20% larger viral load drop than the investigational drug in the various scenarios (1-4), (Figure 7).

The competitor was compared against the investigated drug once for each scenario. The null hypothesis stated that the investigated drug and the competitor did not differ in terms of INH. Number of subjects in each arm needed to reach 80 and 90% power was investigated with the MCMP method. The simulation dataset consisted of 2500 individuals in each arm. For comparison, the power to detect a difference in the viral load from baseline and day 10 between the investigated drug and the competitor in any of the four scenarios was calculated based on a two-sided, unpaired t-test ($p \leq 0.05$).

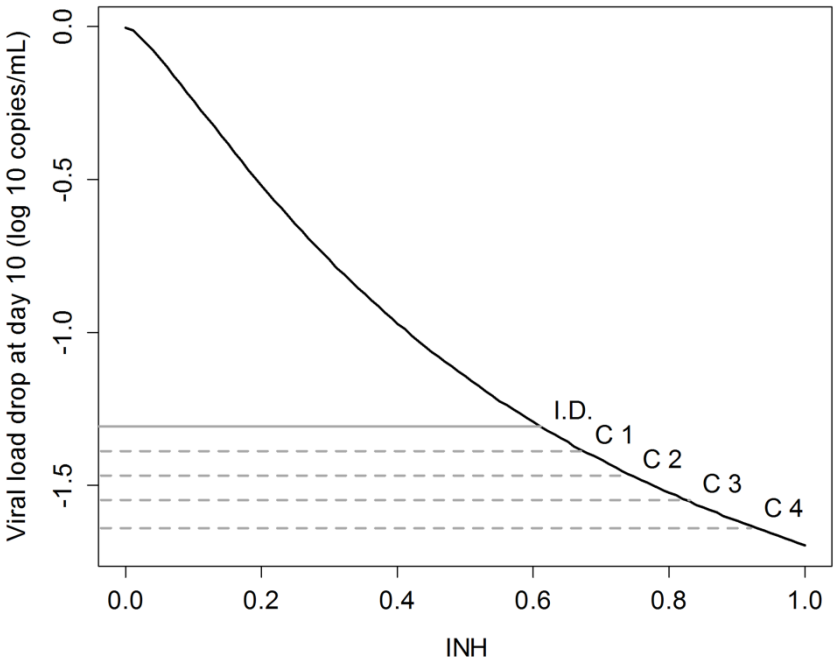

Figure 7. Viral load drop at day 10 of monotherapy verses drug effect (INH). The solid black line is the predicted response curve for all levels of INH. The solid grey line is the investigational drug (I.D.); the grey dashed lines the competitor (C) resulting in 5, 10, 15 and 20% larger drops in viral load at day 10 than I.D. in the four scenarios (1-4).

Simulations and re-estimation of simulated data were performed using the NONMEM software version 7.12 (152). The MCMP methods as well as the SSE method implemented in PsN version 3.4 were used (151,159). Xpose (154) and Piraña (157) was used for handling of model and model output files. Power calculations based on the t-test and ANOVA was computed using the pwr package implemented in R (2.14.1).

7 RESULTS

7.1 Efavirenz and rifampicin (Paper I)

The IVIVE model adequately predicted efavirenz disposition and its interindividual variability after a single dose and at steady state (Figure 8). Prediction was improved when the frequency of poor metabolizers was matched to the observed frequency in the emulated study (39) (Figure 8, bottom). At steady state, efavirenz CL/F was predicted to 9.9 L/h, in close agreement to the observed literature estimate of 9.4 L/h (39).

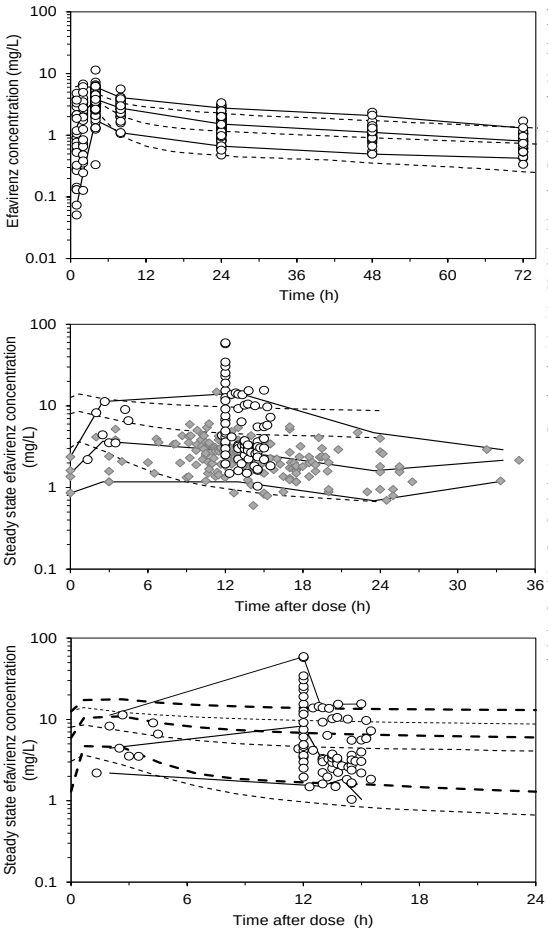

Figure 8 Simulated and observed efavirenz concentration-time profiles after single (top) and repeated (middle and bottom) dosing of 600 mg. The full lines represent the mean and 5th and 95th percentile of the observed systemic concentration. The dashed lines represent the mean and 5th and 95th percentile of the predicted systemic concentrations in 100 simulated individuals. The circles in top figure represent observed concentrations from a single dose study in Ugandan patients (38). The circles (middle and bottom) and diamonds (middle) represent observed plasma concentrations from Zimbabwean and Swedish/Norwegian patients respectively (39,94). In the top and the middle figures a default frequency of slow CYP2B6 metabolizers (11 %) is assumed. In the bottom figure the bold and narrow dashed lines represent Simcyp predictions with frequencies of poor metabolizers of 71 and 11 %, respectively.

The influence of rifampicin on efavirenz clearance at steady state was somewhat underpredicted (12.6 L/h) compared to the literature estimate (17.2 L/h) (160). The reduction in efavirenz exposure at steady state in presence of rifampicin was predicted at 16% [95% CI: 13-19] in agreement with literature estimates 22% (50).

Simulations of an efavirenz dose increment in presence of rifampicin for extensive and slow CYP2B6 metabolizers, above or below 50 kg bodyweight, are depicted in Figure 9. Extensive metabolizers (>50 kg), predicted to have the lowest efavirenz exposure (AUC), were predicted to have the largest decrease in efavirenz AUC due to rifampicin induction, Figure 9. When the efavirenz dose was increased to 800 mg and rifampicin was co-administered the efavirenz AUC normalized to levels observed when 600 mg efavirenz is given without the influence of rifampicin. Slow metabolizers under 50 kg were predicted to have the largest exposure to efavirenz. That exposure increased even further when efavirenz dose was adjusted to 800 mg with concomitantly administered rifampicin.

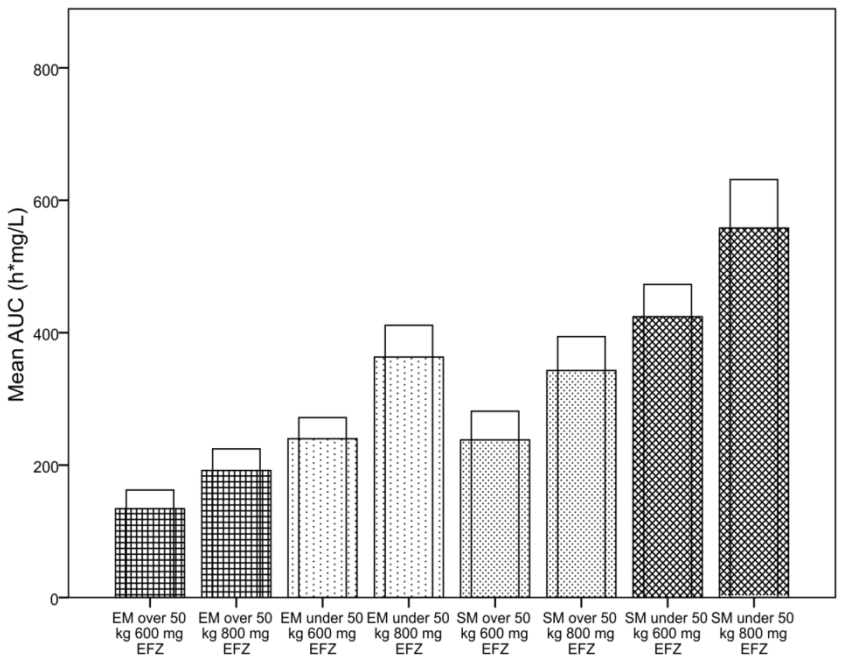

Figure 9. Simulated mean efavirenz steady state AUC with and without concomitant rifampicin grouped according to bodyweight and CYP2B6 phenotype. The open bars show the median efavirenz steady state AUC without concomitant rifampicin while the shaded bars show the median efavirenz steady state AUC when co-administered with rifampicin.

7.2 Efavirenz pharmacokinetics and HIV/AIDS (Paper II)

Single dose efavirenz pharmacokinetics in HIV/AIDS patients and healthy volunteers were described by a two compartment model with the absorption described by transit compartments. The additive part of the combined additive and proportional residual model was study specific. Final model parameters are tabulated in Table 4. Although multiple covariates were identified in the forward inclusion step, only two remained after the backward deletion step. Females were estimated to have a 108% (95% CI: 53-163) increase in peripheral volume of distribution compared to males. The increased volume of distribution resulted in doubling of the terminal half-life in females, Table 5. HIV/AIDS patients were estimated to have 30% (95% CI: 19-41) lower relative bioavailability (F_{rel}) compared to healthy volunteers. The inclusion of sex and disease status as covariates reduced the unexplained variability in V_p and F_{rel} from 48 to 20% and 30 to 21%, respectively. When adjusted for difference in F_{rel} and body weight, CL/F was estimated at 3.73 and 5.31 L/h for a 70 kg healthy volunteer and HIV/AIDS patient, respectively.

Table 4. Parameter estimates for the final model, scaled to a 60 kg subject.

Parameter	**Estimate [RSE %]**	**IIV CV % [RSE %]**
CL/F (L/h)	3.32 [6.51]	17.7 [29.6]
V_c /F(L)	21.9 [23.8]	115.0 [16.9]
V_p /F(L)	149 [9.33]	19.7 [46.8]
Effect of sex on V_p/F (L) (females compared to males)	+108% [26.9]	
Q/F (L/h)	21.4 [10.6]	0 (fixed)
k_a(h^{-1})	0.248 [16.3]	45.3 [14.5]
MTT(h^{-1})	1.11 [12.0]	78.0 [11.8]
NN(n)	6.52 [17.3]	0 (fixed)
F_{rel}	1 (fixed)	20.9 [29.1]
Effect of HIV/AIDS on F_{rel} (Patients compared to healthy volunteers)	-29.7 [19.0]	
Proportional residual error (CV %)	14.2 [11.1]	
Additive residual error patients (mg/L)	0.28 [13.7]	
Additive residual error healthy volunteers (mg/L)	0.12 [24.8]	

CL/F: oral clearance, CV: coefficient of variation, F_{rel}: relative bioavailability, which was fixed at 1 in healthy subject, IIV: interindividual variability, k_a: first- order absorption rate constant, MTT: mean transit time, NN: estimated number of theoretical transit absorption compartments, Q/F: intercompartmental clearance, RSE: relative standard error, V1/F: volume of distribution of the central compartment after oral administration, V2/F: volume of distribution of the peripheral compartment after oral administration.

Table 5. Secondary parameters of the final model for typical male and female subjects.

Parameter	Male		Female	
	Healthy volunteer	HIV/AIDS patient	Healthy volunteer	HIV/AIDS patient
$AUC_{(0\text{-}24\ hours)}$ [a] (h·mg/L)	60	47	48	36
$T_{½}$, [b] (hours)	40	40	78	78

AUC: area under the concentration time curve, $T_{½}$: elimination half-life. [a] Based on median weight: male patients (65 kg), male healthy volunteers (65 kg), female patients (52 kg) and female healthy volunteers (57 kg).[b] Scaled to a 60 kg subject.

7.3 Atazanavir and bilirubin (Paper III)

Atazanavir pharmacokinetics were described by a one compartment model with an absorption lag-time (0.96 hours) and absorption rate constant (3.4 $hour^{-1}$), fixed according to literature values (75). The atazanavir concentration-dependent inhibition of bilirubin elimination was described by an indirect response model type II (161). In Equation 18: B denotes the bilirubin concentration in blood, k_{in} is the zero-order constant for bilirubin production, and k_{out} is first-order elimination rate constant of bilirubin. The first order elimination constant (k_{out}) of bilirubin was inhibited by atazanavir plasma concentration (C_p) by E_{inh}, according to Equation 19.

$$\frac{dB}{dt} = k_{in} - k_{out} \cdot [1 - E_{inh}] \cdot B \qquad \text{Equation 18}$$

$$E_{inh} = \frac{I_{max} \cdot C_p}{IC_{50} + C_p} \qquad \text{Equation 19}$$

The fraction of inhibition is dependent on the maximum possible inhibition I_{max}, C_p and the concentration of atazanavir resulting in 50% of I_{max} (IC_{50}). Parameters of the final model are tabulated in Table 6. The average steady state concentration of atazanavir was estimated at 2.75 µmol/L and resulted in an 82% inhibition of k_{out}. The elimination half-life of bilirubin was estimated at 8.2 hours (range: 5.4-10.8 hours), based on the average, minimum and maximum atazanavir concentration at steady state for the typical patient. The inhibited and uninhibited bilirubin half-lifes were computed with Equation 20. The E_{inh} was fixed to 0 in the uninhibited case. The uninhibited bilirubin half-life (1.64 hours) was in the same magnitude as estimates of the dominant beta phase half-life of radiolabeled bilirubin found in the literature, 1.16 hours (155).

$$t_{½} = \frac{\ln 2}{k_{out} \cdot [1 - E_{inh}]} \qquad \text{Equation 20}$$

7.3.1 Simulations of non-adherence (Deterministic)

Deterministic simulations with the typical parameter estimates of the final model were used to investigate the influence of non-adherence on the bilirubin concentration in blood. A single missed dose of atazanavir resulted in average bilirubin concentration decrease from 35 to 13 µmol/L. Two and three consecutive missed doses resulted in a bilirubin concentration close to (8.2 µmol/L) or at the estimated baseline level (7.8 µmol/L). The simulation model above was used to simulate an atazanavir pharmacokinetic profile resulting in C_{trough} at the MEC of 0.2 µmol/L. The bilirubin trough concentrations for that specific atazanavir PK profile were then simulated. Bilirubin concentrations at various baseline concentrations versus bilirubin trough concentrations constitute the proposed nomogram, Figure 10. The black area represents results from individuals with suboptimal atazanavir exposure (below MEC), while the white area represents bilirubin concentration corresponding to atazanavir exposure above MEC.

Table 6. Parameter estimates of the final pharmacokinetic and pharmacodynamic models describing atazanavir and its influence on bilirubin in HIV/AIDS patients.

	Parameter	Estimate (95% CI)	IIV, %CV (RSE %)
PK model	Lag-time (h)	0.96[a]	
	k_a (h^{-1})	3.4[a]	
	V/F (L)	93.6 (62-125)	53.1 (43.6)
	CL/F (L/h)	6.47 (5.39-7.55)	43.8 (19.5)
	Correlation		
	p(CL/F, V/F)	0.290	
	Residual error		
	σ_{prop} (%)	51.0 (42.7-59.3)	
PD model	Baseline (µmol/L)	7.69 (6.99-8.39)	32.6 (20.2)
	k_{out} (h^{-1})	0.420 (0.36-0.48)	
	I_{max} (%)	91.0 (87-94)	
	IC_{50} (µmol/l)	0.30 (0.24-0.37)	
	Residual error		
	σ_{prop} (%)	39.4 (35.5-43.3)	
	σ_{add} (µmol/l)	2.39 (1.96-2.82)	

k_a: absorption rate constant, V/F: volume of distribution, CL/F: clearance, p: correlation coefficient, σ_{prop}: proportional residual variability, k_{out}: fractional turnover rate, I_{max}: maximum inhibition constant, IC_{50} concentration resulting in 50% of Imax, σ_{add}: additive residual error, IIV: inter-individual variability. [a] fixed according to (75).

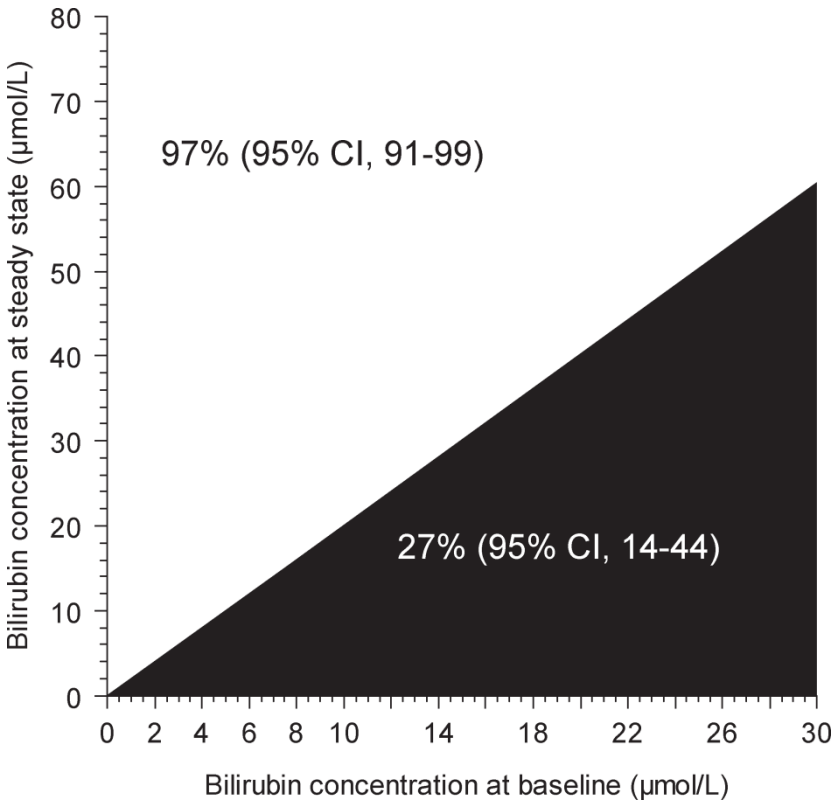

Figure 10. The atazanavir-bilirubin nomogram. The black area represents bilirubin steady state levels associated with atazanavir exposure below the minimal effective concentration (MEC) of 0.2 µmol/L. The white area represents bilirubin levels associated with atazanavir concentrations over MEC. Results of the external validation are superimposed on the nomogram. The percentages and the confidence intervals (95% CI) in the white and the black area represent the probability of nomogram to be correct when predicting an observation to be above or below MEC, respectively, results from Paper IV.

7.4 Validation of the atazanavir bilirubin nomogram (Paper IV)

The nomogram was validated in three external cohorts on a ritonavir boosted atazanavir based HAART regiment. The data from the cohorts is superimposed on the nomogram in Figure 11. The predictive properties of the nomogram are shown in Table 7. In general, the nomogram showed high probability of predicting a negative result when the atazanavir concentration is truly over MEC (specificity: 91% [95% CI: 87-94]). The negative predictive value i.e. the probability

of a true negative result for all observations characterized as over MEC, was also high (NPV: 97% [95% CI: 95-99]). The positive predictive value was lower than NPV for all cohorts, especially so for the Italian cohort on a ritonavir boosted atazanavir treatment. This is due to the high number of false positive samples in the Italian cohort compared to the others (Figure 11 C).

The nomogram was also validated in an Italian cohort on an unboosted atazanavir based HAART treatment. The predictive properties of the nomogram in terms of NPV were significantly lower in the unboosted compared to the boosted cohorts ($NPV_{unboosted}$: 70% [95% CI: 57-80] versus $NPV_{total\ boosted}$: 97% [95% CI: 95-99]). NPV and PPV for the combined analysis of all cohorts on a ritonavir boosted atazanavir regiment are shown in the white and the black area of the nomogram in Figure 10, respectively.

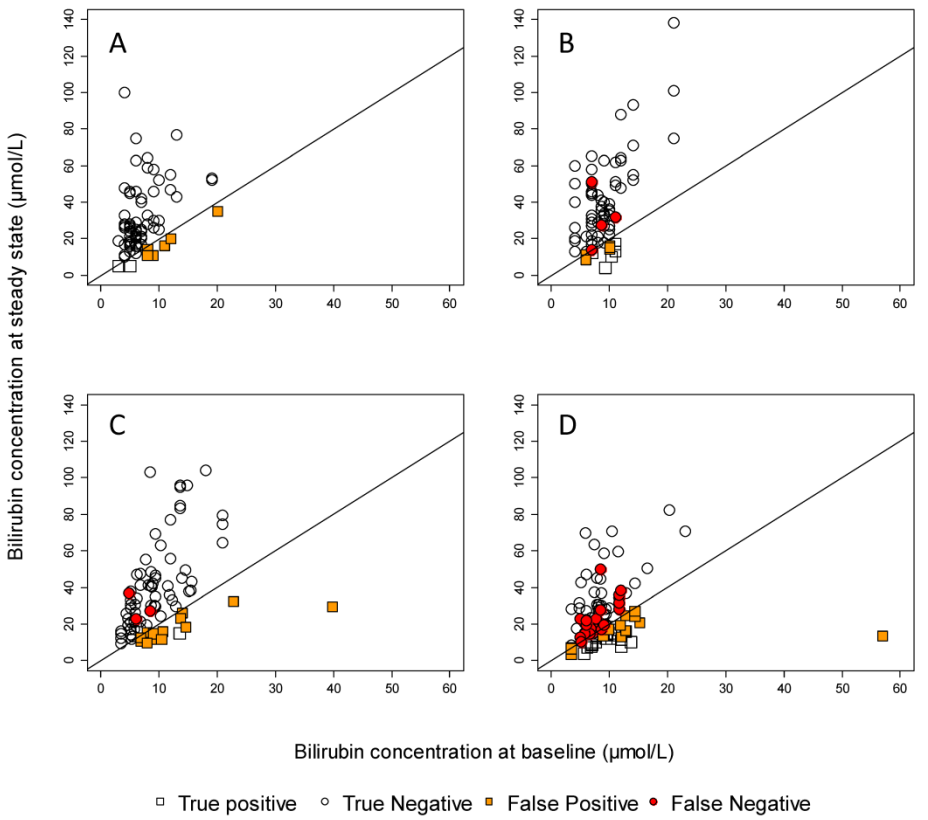

Figure 11. The bilirubin nomogram applied on Norwegian (A), French (B), ritonavir boosted Italian (C) and unboosted Italian (D) patients. Observations below the full line are predicted to correspond to atazanavir concentrations below the minimal effective concentration (MEC) of 0.2 µmol/L (150 ng/ml). The white and the colored points denote correct and incorrect predictions, respectively.

Table 7. Summary of the bilirubin nomogram's predictive properties in various HIV-1 patient populations

	Italian		**French**		**Norwegian**		**Total**	
	Boosted ATZ		*Boosted ATZ*		*Boosted ATZ*		*Boosted ATZ*	
Parameter	Value	95% CI	Value	95% CI	Value	95% CI	Value	95% CI
Specificity	0.81	(0.71-0.89)	0.95	(0.91-0.99)	0.92	(0.85-0.97)	0.91	(0.87-0.94)
Sensitivity	0.25	(0.01-0.80)	0.55	(0.21-0.86)	1	(0.28-1.00)	0.59	(0.33-0.82)
Accuracy	0.79	(0.68-0.87)	0.93	(0.87-0.97)	0.93	(0.86-0.97)	0.89	(0.85-0.92)
PPV	0.06	(0.002-0.3)	0.5	(0.19-0.81)	0.36	(0.11-0.69)	0.27	(0.14-0.44)
NPV	0.96	(0.88-0.99)	0.97	(0.92-0.99)	1	(0.94-1.00)	0.97	(0.95-0.99)

PPV: positive predictive value, NPV: negative predictive value, CI: Confidence interval, ATZ: atazanavir

7.4.1 Simulation of non-adherence (Stochastic)

Two methods for predicting non-adherence were evaluated using the previously developed stochastic PKPD model (Paper III). Method one was based on the nomogram and method two was based on direct measurement of the atazanavir plasma concentration. Figure 12 shows the performance metrics of the nomogram and the direct plasma measurements. There was no difference in the performance in the three scenarios. There were, however, large differences in performance between the different sampling events. In terms of NPV: at Event1a, direct atazanavir measurement was slightly better than the nomogram although both methods performed adequately with NPV >98%. At event 2, the nomogram and direct atazanavir measurement performed equally. At Event 1b, where the patient is trying to conceal the period of non-adherence by taking an atazanavir dose 1 hour before sampling, the nomogram had a significantly higher NPV than direct atazanavir measurement. In terms of PPV, direct atazanavir measurement predicted non-adherence well at Event 1a and 1b. At Event 2, both the methods showed poor performance. Performance metrics for all scenarios and event are shown in Figure 12.

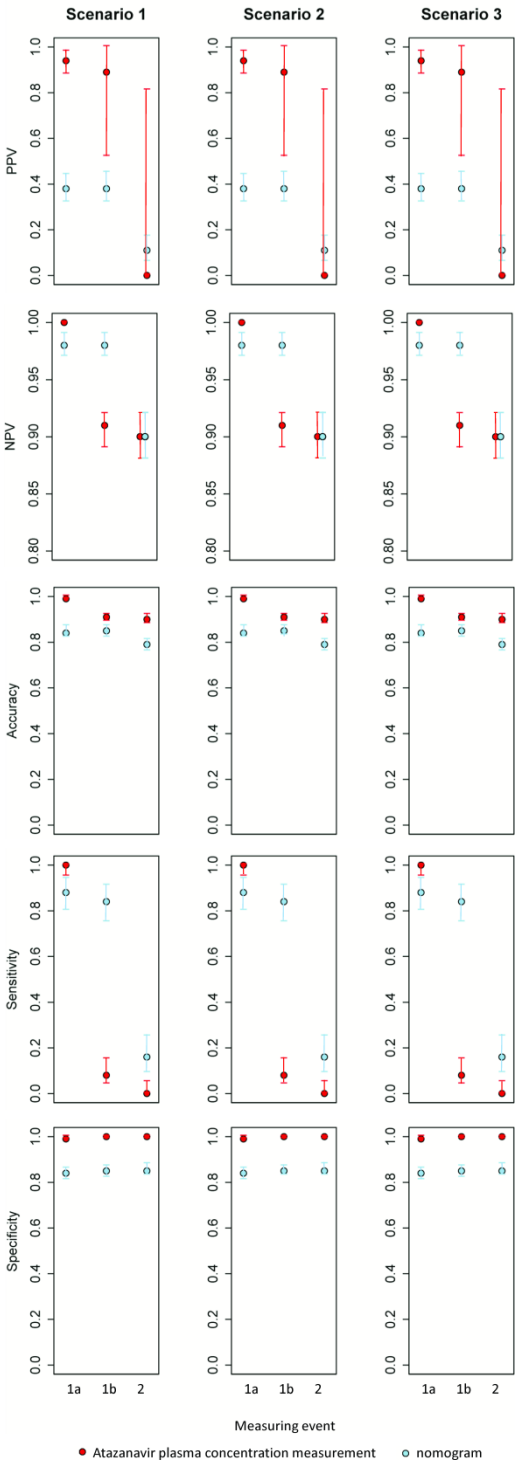

Figure 12. Summary of predictive properties of the bilirubin nomogram (circles) and atazanavir drug monitoring (triangles) based on simulations of 1000 virtual patients. The circles represent median while the bars represent the 95% confidence interval. Colors red and blue represent the atazanavir concentration measurement and bilirubin, respectively. PPV: positive predictive value, NPV: negative predictive value. The scenarios and the events are explained in the methods section.

7.5 Phase II HIV-1 trials (Paper V)

A simulation of the dose-response relationship for each of the tested doses is shown in Figure 13. The mean (±SD) drop in viral load at day 10 was 0.31 (±0.31), 0.85 (±34), 1.38 (±0.32) and 1.56 (±0.30) $\log_{10}$ copies/mL for the tested doses. Using the model based approach, 5 patients (1 per arm) was sufficient to detect a significant dose-response relationship in the POC/dose-finding trial with >99% power. To reach >99% power based on the t-test where the highest dose is compared to the placebo arm, 15 patients (3 per arm) were required. The same sample size (3 patients per arm) was required using ANOVA where the mean viral load drop at day 10 for all arms is compared (Table 8).

The sample size of 5 patients (1 per arm) resulted in insufficient precision in ED_{50} (relative standard error [RSE]: 45.2%), based on SSE (1000 samples). A sample size of 3 patients per arm is necessary to estimate ED_{50} with reasonable bias (5.4%) and precision (RSE: 25.7%).

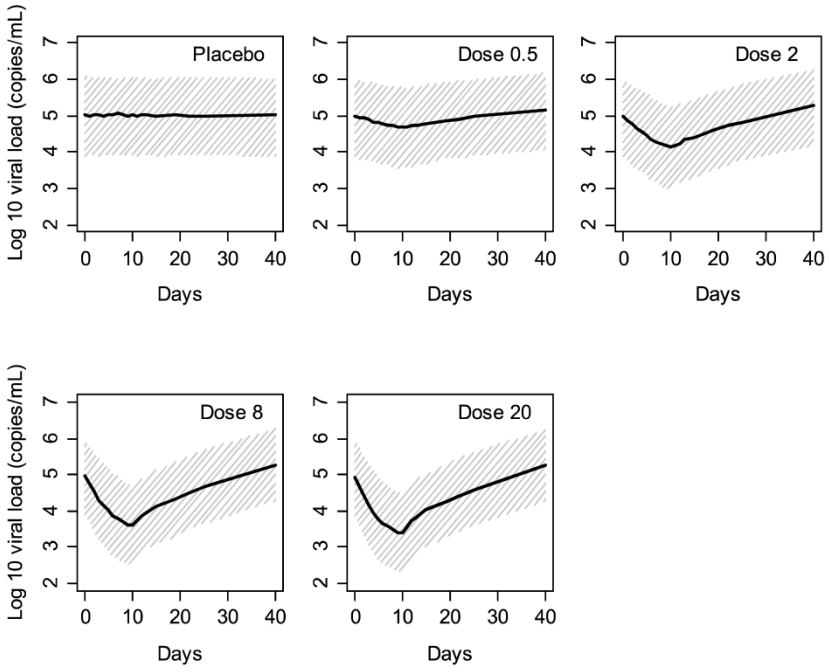

Figure 13. The simulated dataset used for power calculations of the POC trial with the MCMP method. The panels represent the tested doses including placebo; the solid black line is the median; the grey area is the 90% prediction interval; 1000 individuals are simulated in each arm.

Table 8. Total sample size and power for showing a dose-response relationship for the model based drug development approach (MBDD) and the traditional statistical approach (two-sided, unpaired t-test and ANOVA) for a 5 armed (including placebo) trial design. Numbers in parenthesis are number of patients per arm.

Power (%)	MBDD	t-test lowest dose	t-test highest dose	ANOVA
80	5 (1)	85 (17)	10 (2)	10 (2)
90	5 (1)	115 (23)	15 (3)	15 (3)
99	5 (1)	195 (39)	15 (3)	15 (3)

Results from the comparison of a hypothetical investigational drug against the active competitor in the four scenarios are shown in Figure 14. The smallest difference in treatment effect that is possible to detect, with 80% power, using the MBDD approach and a sample size of 20 (10 patients per arm) is 20%. The treatment effect is here defined as drop in viral load at day 10 of monotherapy. Using a t-test a sample size of 68 patients (34 per arm) is required to detect the same effect size with 80% power, Figure 14. The difference in required sample size for the t-test and the MBDD approach and was 3.4, 3.9, 3.3, and 3.3 fold for a difference in effect of 20, 15, 10 and 5%.

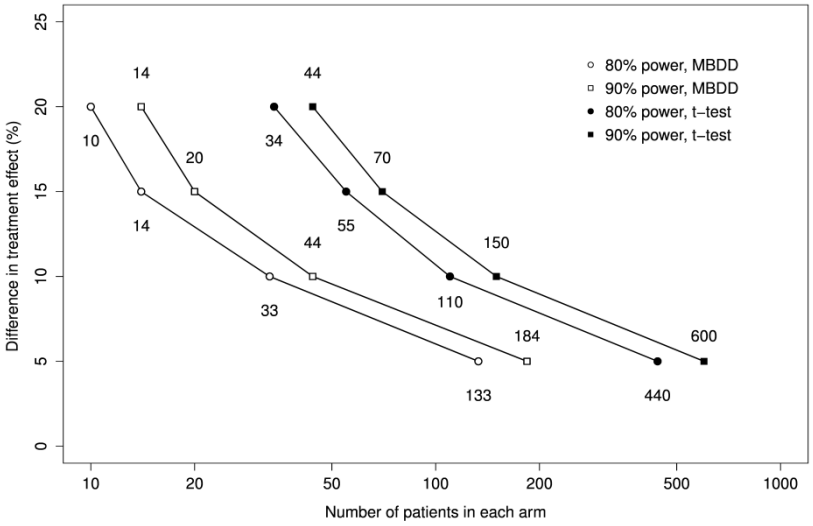

Figure 14. Number of patients per arm (2 arms) needed to detect various differences in treatment effect between the investigated compound and active competitors at 80% (circles) and 90% (squares) power based on a Model Based Drug Development approach (MBDD) and two-sided unpaired t-test, respectively.

8 DISCUSSION

The father of modern medicine, Sir William Osler (1849-1919) once said: “The good physician treats the disease; the great physician treats the patient who has the disease.” Today we refer to this approach as personalized medicine. This thesis aims to optimize and individualize antiretroviral pharmacotherapy for the treatment of HIV-1 infection by investigating various aspects of the treatment such as drug-drug interaction, disease effect on pharmacokinetics and drug concentration monitoring. The pharmacotherapy in resource limited settings has been given special emphasis throughout most of the papers in this thesis. In addition the thesis exemplifies how the development of new treatment options and clinical drug development programs can be informed and expedited using pharmacometrics and model based tools.

In paper I, the most appropriate action is investigated when a CYP P450 inducing drug (rifampicin) is given concomitantly to an efavirenz-containing antiretroviral regiment. Previous dosage recommendations counteracting this interaction were based on inadequate clinical support. Furthermore, the FDA encouraged *in silico* simulations to evaluate current recommendations (52). By use of *in silico* methods (IVIVE), which rely solely on non-human data, various doses were tested on different virtual subpopulations, e.g. slow and extensive metabolizers as well as patients below or above 50 kg of body weight. The results indicated that the recommended efavirenz dose increment in patients over 50 kg bodyweight is appropriate in presence of rifampicin. The methodology used allowed a virtual study to be conducted avoiding a large clinical trial in a not easily recruited population (slow metabolizer, <50 kg), saving considerable time and resources. Additionally, the IVIVE method also allowed virtual investigation of appropriate doses without any risks to patients. This concept is potentially of great use in phase I of drug development where it can aid the prediction of exposure in man as well as predict drug-drug interactions based on preclinical data.

The immune system of HIV-1 infected patients is under severe strain which can ultimately lead to the immunodeficiency syndrome known as AIDS. Opportunistic infections and virus induced cancers may require the patients to be treated with multiple concomitant drugs, increasing the risk of metabolic drug-drug interactions. Drug-drug interactions can be predicted from *in vitro* data as shown in paper I. It is, however, more common to study the suspected interaction in a clinical trial. Moreover, due to ethical aspects, as well as for other reasons, these trials are often conducted in healthy volunteers rather than in HIV-1 patients. One important assumption is that the pharmacokinetics of the interacting drugs does not differ between patients and healthy volunteers. That assumption is challenged in paper II where difference in efavirenz pharmacokinetics between

healthy volunteers and HIV-1 patients were investigated by NLME. Any substantial difference in exposure between patients and healthy volunteers may lead to under- or overprediction of the investigated interaction. The results in paper II show that patients have approximately 30% lower exposure than healthy volunteers which demonstrates the need of clinical trials in the target population rather than in healthy volunteers. In addition to drug-drug interaction trials, potential difference in exposure between healthy volunteers and patients can be of importance in all phase I trials conducted in healthy volunteers. Caution should be taken when results from healthy volunteers are extrapolated to the target populations that can potentially differ in exposure.

Aside from drug-drug interactions, other factors may lead to suboptimal exposure in patients e.g. non-adherence. The large pill burden associated with the pharmacotherapy of HIV-1 and the treatment of other concomitant infections and conditions may decrease patients motivation to adhere to therapy (162) and thus affect patients' drug exposure. As adherence is an important cause of treatment success, regular assessment and documentation of adherence are recommended (13).

Drug exposure can be directly determined by measuring the drug concentration in plasma i.e. therapeutic drug monitoring. Unfortunately this approach requires access to costly equipment as well as highly trained personnel. Additionally it may take considerable time for the sample to be analyzed and interpreted. These obstacles may pose a challenge, especially so in resource limited settings. The atazanavir-bilirubin nomogram in Paper III was developed with these obstacles in mind.

Hyperbilirubinemia is caused by atazanavir concentration-dependent inhibition of bilirubin conjugation. The nomogram itself is a practical adaptation of a semi mechanistic nonlinear mixed effects model of that inhibition. Bilirubin concentration measurements are required for the use of the nomogram. These can be obtained using an inexpensive bilirubin meter that can be operated with minimal training. Recent bilirubin meter models are handheld, trans-cutaneous and battery powered, eliminating the need of a continuous power source. Trans-cutaneous and plasma measurements of bilirubin have been shown to be well correlated (163). The use of transcutaneous, battery powered bilirubin meters can in a matter of seconds inform the clinician about a patient's atazanavir exposure without the need of hospital settings.

The nomogram was successfully validated in three external patient populations from Italy, France and Norway, Paper IV, where the credibility of the negative observations was high (NPV: 97% [95% CI: 91-99]). Additional simulations showed that the nomogram could detect ongoing non-adherence in patients. The atazanavir-bilirubin nomogram offers clinicians a valuable, rapid, accurate, inexpensive and easy to use tool to access suboptimal exposure in patients whatever the cause.

Patients and clinicians depend on the resources of the pharmaceutical industry to develop safe and efficacious medicines. These resources are not endless and need to be used rationally. Investigational drugs that are not likely to reach the market need to be discontinued as early as possible so that resources can be redirected towards other projects. To achieve this, clinical trials need to be designed and analyzed using all available knowledge about the disease and the drug so that development teams can make informed decisions about the future of the investigational drug. The knowledge about the drug and the disease should preferably be as integrated as possible e.g. a mechanistic mathematical representation of the drug-disease interaction. In Paper V, a simplified mathematical representation of HIV-1 and CD4 cells and their interaction is used to explore the settings of Phase II monotherapy HIV-1 trials. Two main questions were investigated: 1) can the number of patients required to show a significant dose response relationship be reduced using a MBDD approach, compared to traditional analysis (t-test/ANOVA) and 2) can additional knowledge be gained about the investigational drug's performance relative to competitors, within the fixed design of phase II monotherapy trials (with regards to sample size and study duration). Knowledge about an investigational drug's performance against competitors on the market or in development can be used to inform decisions about future development of that compound. By reducing study size or by increasing knowledge about a drugs performance at an early stage of drug development, costs can be reduced. Additionally, effective use of clinical trials can reduce the number of patients treated with an investigational drug with possible unknown adverse effects.

In conclusion this thesis demonstrates the utility of pharmacometric tools as implemented in model based drug development as well as in optimization of existing therapies for the HIV-1 infection. This is exemplified from various angles e.g. prediction of exposure and drug-drug interactions, disease influence on pharmacokinetics, development and validation of biomarkers as well as optimizing design and analysis of clinical studies.

9 CONCLUSION

The general conclusions of this thesis are that pharmacometric methods can improve the pharmacotherapy of the HIV-1 infection as well as expedite clinical drug development. This is exemplified from various angles in the five Papers that constitute this thesis.

The specific findings were:

- Efavirenz dose should be increased to 800 mg when concomitantly administered with rifampicin in patients above 50 kg of bodyweight.

- Results from drug-drug interactions in healthy volunteers where efavirenz is the perpetrator may be confounded by the difference in efavirenz relative bioavailability (F_{rel}) between healthy volunteers and HIV/AIDS patients. HIV/AIDS patients had 30% lower F_{rel} than healthy volunteers.

- The atazanavir concentration-dependent inhibition of bilirubin conjugation was described by a semi mechanistic nonlinear mixed effects model. A nomogram aimed to predict suboptimal atazanavir/r exposure in patients was created based on the developed model.

- The atazanavir-bilirubin nomogram was validated in several external populations. Further, it offers clinicians a rapid, accurate, inexpensive and easy to use tool to access suboptimal exposure and non-adherence in patients whatever the cause.

- Model based hypothesis testing allows a 3-fold reduction in sample size for proof of concept in HIV-1 II monotherapy trials.

- Compared to traditional hypothesis testing, model based hypothesis testing required 3.4-fold smaller sample size to detect a difference of 20% or more in treatment effect in phase II HIV-1 monotherapy trials.

ACKNOWLEDGEMENT

The work presented in this thesis was carried out at the Unit for Pharmacokinetics and Drug Metabolism at the Department of Pharmacology, Institute of Neuroscience and Physiology, Sahlgrenska Academy at the University of Gothenburg.

I thank Professor Michael Ashton for unlocking my passion for pharmacokinetics which later evolved to include pharmacometrics and drug development. Your introduction of the pharmacokinetics' courses at the very first day of the pharmacy program in 2003 made me exited of things to come. Almost four years later I finally got the chance to explore the intricate world of pharmacokinetics; needless to say, I was not disappointed. Further, I thank you for accepting me to the PKDM group as a PhD student and allowing me play in the PK playground as well as giving me the chance to freely pursuit my passion for pharmacometrics and drug development.

I also thank my co-adviser Dr. Daniel Röshammar who has often been the trailblazer and for always successfully trying out new management techniques on me. When I thought I did not have more to give you motivated me to take it one step further. You never lost your faith in me throughout the many revisions of manuscripts. Further, I thank you for including me as "junior" during some of the PAGE adventures, perhaps most notably in St. Petersburg.

Dr. Angela Äbelö, my source of knowledge about the real word and friend, I thank you for easing my burden and offering valuable insight and advice when needed. Professor Magnus Gisslén, my co-adviser is responsible for providing me with much needed clinical context which I thank him for. Dr. Ulrika Simonsson, I thank you for always sharing your enthusiasm and energy.

This journey has been made easier with past and current members of the PKDM unit. Some of you were in addition to colleagues my teachers as well. In no particular order; I am grateful for your contributions, Richard, "the Umpa Lumpa of science", Höglund my long time officemate, for always making time to discuss problems. Therese Ericsson for your inspirational work ethic. Sofia, "Iron Man", Birgersson for sometimes letting a frog or two slide by and for inspiring the phrase "Sofia pants". Carl, "the Anglophile", Johansson for your ability to know more than I about things I care about and for not letting any frogs slide by unnoticed. Dr. Joel, "Dr. Dice" Tärning, for his transformation from a teacher to a friend and for welcoming me as a guest in his team and home in Bangkok. I thank you for the PAGE adventures in St. Petersburg, Berlin, Venice and all the other times we decided it was time to lay of the science and find the nearest watering hole. Dr. Rasmus Jansson

Löfmark, my officemate for a brief period of time, for your superior knowledge in PKPD and kind words to a young and overly confident PhD student. At least I am not so young any more. Emile Bienvenu, your work ethic and ability to overcome unbearable challenges makes me humble. Betty Njau, your wonderful smile and honesty. Dr. Sofia Friberg Hietala and Dr. Sara Asimus I thank for your part in inspiring me to join the PKDM unit. Karin Saalman and Helena Andersson née Dahlqvist, thank you for the time you spent at the unit. Oskar Clewe and Helena Andersson "my" master students, I thank you for your extraordinary good work. Not ruining pharmacometrics for you two is possibly my greatest achievement. Dr. Elin Karlsson, the newest senior member of the PKDM unit, I wish you much success in science and in shaping of the young pharmacists' minds.

The department of pharmacology was headed by Professor Hans Nissbrandt during most part of my time here. I thank you for always making time for me and your generous contribution to the Rekić family library. Professor Gunnar Tobin, for your contribution to the pharmacy program and for always being kind to the sometimes cheeky young scientist.

Martin, "MC^2", Johnsson, my friend and colleague, it is hard to admit but your passion for science exceeds mine. This is especially hard to admit when you divide your time between science and product/club development. Karin, "*l'Artiste*", Dankis, for your valuable contribution to this thesis and for making Martin a better man. I thank Jakob, "know it all" Näslund for absolutely outperform me in any argument no matter how well a think I know the subject and for being a kind friend at the same time. Erik, "Struler", Studer, for significantly raising Pharmens's hip factor. I am also equally grateful for all other friends at Pharmen and other neighbouring units for the fun times at various social events.

Dr. Martin, "Steamroller" Bergstrand deserves a special salute for the time we shared an apartment in Bangkok. We had some memorable mornings [SIC] exploding the local watering holes. When others endured the young overly confident scientist you encouraged him.

I am grateful to Dr. Wojciech Krzyzanski for accepting me to his lab in Buffalo to do my masters' thesis and all the valuable lessons in modelling as well as experimental pharmacokinetics. Dr. Sihem Ait-Oudhia, I thank you for your friendship, kind words and guidance.

My friends outside of pharmen are responsible for all my interpersonal skills; they are the members of the GU-Nit, in no particular order. Ali "CEO" Kouchek, my dear friend since the seventh grade. From 418, 2ans and shugović to top of the world – my partner in *coup d'état*. Mustafa, "Musse", Matlak, he rose like the phoenix and reclaimed his glory at inferno. I thank you for always being a true friend. Kaveh, "Caveman", Teimori for your friendship, for harbouring me when I was temporarily homeless in Vietnam and for all the other adventures. Samir, "Samy", Dalili, for all the fun sum-

mers in the eselkån. Volkan, “professorn”, Sayin for making me proud to know a real scientist and for watching sci-fi series with me when Sara was in Oslo. Mohamed, “Silky-Moe”, Ibrahim for great times. Milad, “the Poet”, Kouchek for your inspiring willpower. Martin, “Hamsta”, Tamtè for great times and being generous with your bachelor pad. Magnus, “Ma’hgnooos”, Hansen for taking on a bunch of youngsters underneath your wings. My cousin Armin Kalajdzija is always a great source of inspiration and fun! Someone should write a book of all your adventures.

To my dear loving parents, Sead and Jasmina Rekić. Sir Isaac Newton wrote: “If I have seen further it is by standing on the shoulders of giants”. He was referring to other scientist, here, I refer to you. I am proud to be the son of the strongest, most resourceful and inspiring people I have met. I am grateful for your infinite love and kindness as parents. I owe it all to you.

Sara, my love, now I understand why they say words are not enough. You are my best friend and my true love. I am grateful for your smile every morning I wake up. You make life a joy. With you I am forever happy.

THE BEGINNING

REFERENCES

1. Benet LZ. Pharmacokinetics: Basic Principles and Its Use as a Tool in Drug Metabolism. Drug Metabolism and Drug Toxicity. 1984;199.

2. Aarons L. Population pharmacokinetics: theory and practice. British journal of clinical pharmacology. 1991 Dec;32(6):669–70.

3. Barrett JS, Fossler MJ, Cadieu KD, Gastonguay MR. Pharmacometrics: a multidisciplinary field to facilitate critical thinking in drug development and translational research settings. Journal of Clinical Pharmacology. 2008;48(5):632–49.

4. Ette E, Williams PJ. Pharmacometrics: the science of quantitative pharmacology. Am J Pharm Educ. 2007;71(4):75.

5. GLOBAL HIV/AIDS RESPONSE, Epidemic update and health sector progress towards Universal Access, Progress Report 2011 [Internet]. [cited 2012 Oct 22]. Available from: http://whqlibdoc.who.int/publications/2011/9789241502986_eng.pdf

6. Little SJ. Transmission and prevalence of HIV resistance among treatment-naive subjects. Antiviral therapy. 2000 Mar;5(1):33–40.

7. Freed EO. HIV-1 replication. Somatic cell and molecular genetics. 2001 Nov;26(1-6):13–33.

8. Greene W, Peterlin B. Charting HIV's remarkable voyage through the cell: basic science as a passport to future therapy. Nature medicine. 2002;8(7):673–80.

9. Joly V, Jidar K, Tatay M, Yeni P. Enfuvirtide: from basic investigations to current clinical use. Expert opinion on pharmacotherapy. 2010 Nov;11(16):2701–13.

10. Lieberman-Blum SS, Fung HB, Bandres JC. Maraviroc: a CCR5-receptor antagonist for the treatment of HIV-1 infection. Clinical therapeutics. 2008 Jul;30(7):1228–50.

11. Richman DD. HIV chemotherapy. Nature. 2001 Apr 19;410(6831):995–1001.

12. Harris M, Montaner JS. Clinical uses of non-nucleoside reverse transcriptase inhibitors. Reviews in medical virology. 2000;10(4):217–29.

13. Josephson F, Albert J, Flamholc L, Gisslén M, Karlström O, Moberg L, et al. Treatment of HIV infection: Swedish recommendations 2009. Scandinavian journal of infectious diseases. 2009 Jan;41(11-12):788–807.

14. Eshleman S, Guay L, Mwatha A, Cunningham S, Brown E, Musoke P, et al. Comparison of Nevirapine (NVP) Resistance in Ugandan Prophylaxis: HIVNET 012. AIDS Research and Human Retroviruses. 2004;20(6):595–9.

15. Nguyen B-YT, Isaacs RD, Teppler H, Leavitt RY, Sklar P, Iwamoto M, et al. Raltegravir: the first HIV-1 integrase strand transfer inhibitor in the HIV armamentarium. Annals of the New York Academy of Sciences. 2011 Mar;1222:83–9.

16. Freed EO. HIV-1 replication. Somatic cell and molecular genetics. 2001 Nov;26(1-6):13–33.

17. Adams J, Dumond J, Kashuba A, Ernst M. Pharmacotherapy of human immunodeficiency virus infection in Koda-Kimble & Young´s Applied Therapeutics. 10th ed. Alldredge B, Correli R, Ernst M, Guslielmo B, Kradjan W, Williams B, editors. Philadelphia (PA): Lippincott Williams, & Wilkins; 2012. p. 1690–715.

18. Panel on Antiretroviral Guidelines for Adults and Adolescents. Guidelines for the use of an- tiretroviral agents in HIV-1-infected adults and adolescents. [Internet]. Developed by the HHS Panel on Antiretroviral Guidelines for Adults and Adolescents – A Working Group of the Office of AIDS Research Advisory Council (OARAC). 2011 [cited 2011 Nov 28]. p. 1–167. Available from: http://aidsinfo.nih.gov/contentfiles/lvguidelines/adultandadolescentgl.pdf

19. Bangsberg DR. Less than 95% adherence to nonnucleoside reverse-transcriptase inhibitor therapy can lead to viral suppression. Clinical infectious diseases. 2006 Oct 1;43(7):939–41.

20. Rakhmanina NY, van den Anker JN. Efavirenz in the therapy of HIV infection. Expert opinion on drug metabolism & toxicology. 2010 Jan;6(1):95–103.

21. Maggiolo F, Ravasio L, Ripamonti D, Gregis G, Quinzan G, Arici C, et al. Similar adherence rates favor different virologic outcomes for patients treated with nonnucleoside analogues or protease inhibitors. Clinical infectious diseases. 2005 Jan 1;40(1):158–63.

22. Approval documentation for Sustiva ™ (Efavirenz) NDA no 020972, DuPont. 2009;

23. Kim D, Wheeler W, Ziebell R, Johnson J, Prejean J, Heneine W, et al. Prevalence and Consequences of Transmitted Drug Resistance Prevalence of Transmitted Antiretroviral Drug Resistance among Newly-diagnosed HIV-1-infected Persons , US , 2007 [Internet]. CROI 2010. 2010 [cited 2012 Oct 22]. p. #580. Available from: http://retroconference.org/2010/Abstracts/38109.htm

24. Hirsch MS, Günthard HF, Schapiro JM, Brun-Vézinet F, Clotet B, Hammer SM, et al. Antiretroviral drug resistance testing in adult HIV-1 infection: 2008 recommendations of an International AIDS Society-USA panel. Clinical Infectious Diseases. 2008;47(2):266–85.

25. Panel on Antiretroviral Guidelines for Adults and Adolescents. Guidelines for the use of antiretroviral agents in HIV-1-infected adults and adolescents. Developed by the HHS Panel on Antiretroviral Guidelines for Adults and Adolescents – A Working Group of the Office of AIDS Research Advisory Council (OARAC). 2011[cited 2012 Nov 28]. Available from: http://aidsinfo.nih.gov/contentfiles/lvguidelines/adultandadolescentgl.pdf

26. Cypc CPE, Yeh RF, Gaver VE, Patterson KB, Rezk ÞNL, Baxter-meheux F, et al. Lopinavir / Ritonavir Induces the Hepatic Activity of CYP1A2 But Inhibits the Hepatic and Intestinal Activity of CYP3A as Measured by a Phenotyping Drug Cocktail in Healthy Volunteers. In Vitro. 2006;42(1):52–60.

27. Bristol-Myers Squibb. Stocrin (efavirenz) product information leaflet [Internet]. 2011 [cited 2012 Jan 30]. Available from: http://packageinserts.bms.com/pi/pi_sustiva.pdf

28. Lamorde M, Byakika-Kibwika P, Tamale WS, Kiweewa F, Ryan M, Amara A, et al. Effect of Food on the Steady-State Pharmacokinetics of Tenofovir and Emtricitabine plus Efavirenz in Ugandan Adults. AIDS research and treatment. 2012 Jan;2012:105980.

29. Mutlib AE, Chen H, Nemeth GA, Markwalder JA, Seitz SP, Gan LS, et al. Identification and characterization of efavirenz metabolites by liquid chromatography/mass spectrometry and high field NMR: species differences in the metabolism of efavirenz. Drug metabolism and Disposition. 1999;27(11):1319–33.

30. Desta Z, Saussele T, Ward B, Blievernicht J, Li L, Klein K, et al. Impact of CYP2B6 polymorphism on hepatic efavirenz metabolism in vitro. Pharmacogenomics. 2007;8(6):547–58.

31. Ward BA, Gorski JC, Jones DR, Hall SD, Flockhart DA, Desta Z. The cytochrome P450 2B6 (CYP2B6) is the main catalyst of efavirenz primary and secondary metabolism: implication for HIV/AIDS therapy and utility of efavirenz as a substrate marker of CYP2B6 catalytic activity. J Pharmacol Exp Ther. 2003;306(1):287–300.

32. Ogburn ET, Jones DR, Masters AR, Xu C, Guo Y, Desta Z. Efavirenz Primary and Secondary Metabolism In Vitro and In Vivo: Identification of Novel Metabolic Pathways and Cytochrome P450 2A6 as the Principal Catalyst of Efavirenz 7-Hydroxylation. Drug Metabolism and Disposition. 2010;38(7):1218.

33. Bae SK, Jeong Y-J, Lee C, Liu K-H. Identification of human UGT isoforms responsible for glucuronidation of efavirenz and its three hydroxy metabolites. Xenobiotica; the fate of foreign compounds in biological systems. 2011 Jun;41(6):437–44.

34. Faucette SR, Zhang TC, Moore R, Sueyoshi T, Omiecinski CJ, LeCluyse EL, et al. Relative activation of human pregnane X receptor versus constitutive androstane receptor defines distinct classes of CYP2B6 and CYP3A4 inducers. J Pharmacol Exp Ther. 2007;320(1):72–80.

35. Hariparsad N, Nallani SC, Sane RS, Buckley DJ, Buckley AR, Desai PB. Induction of CYP3A4 by efavirenz in primary human hepatocytes: comparison with rifampin and phenobarbital. Journal of clinical pharmacology. 2004 Nov;44(11):1273–81.

36. Cabrera SE, Santos D, Valverde MP, Domínguez-Gil A, González F, Luna G, et al. Influence of the cytochrome P450 2B6 genotype on population pharmacokinetics of efavirenz in human immunodeficiency virus patients. Antimicrobial agents and chemotherapy. American Society for Microbiology (ASM); 2009 Jul;53(7):2791–8.

37. Sánchez A, Cabrera SE, Santos D, Valverde MP, Fuertes A, Domínguez-Gil A, et al. Population Pharmacokinetic/Pharmacogenetic Model in Caucasian Hiv-Infected Patients for Optimization of Efavirenz Therapy. Antimicrobial agents and chemotherapy. 2011 Sep 6;55(11):5314–24.

38. Mukonzo JK, Röshammar D, Waako P, Andersson M, Fukasawa T, Milani L, et al. A novel polymorphism in ABCB1 gene, CYP2B6*6 and sex predict single-dose efavirenz population pharmacokinetics in Ugandans. Br J Clin Pharmacol. 2009;68(5):690–9.

39. Nyakutira C, Röshammar D, Chigutsa E, Chonzi P, Ashton M, Nhachi C, et al. High prevalence of the CYP2B6 516G-->T(*6) variant and effect on the population pharmacokinetics of efavirenz in HIV/AIDS outpatients in Zimbabwe. Eur J Clin Pharmacol. 2008;64(4):357–65.

40. Ribaudo HJ, Liu H, Schwab M, Schaeffeler E, Eichelbaum M, Motsinger-Reif A a, et al. Effect of CYP2B6, ABCB1, and CYP3A5 polymorphisms on efavirenz pharmacokinetics and treatment response: an AIDS Clinical Trials Group study. The Journal of infectious diseases. 2010 Sep 1;202(5):717–22.

41. Wang J, Sönnerborg A, Rane A, Josephson F, Lundgren S, Ståhle L, et al. Identification of a novel specific CYP2B6 allele in Africans causing impaired metabolism of the HIV drug efavirenz. Pharmacogenetics and genomics. 2006 Mar;16(3):191–8.

42. Mehlotra RK, Ziats MN, Bockarie MJ, Zimmerman P a. Prevalence of CYP2B6 alleles in malaria-endemic populations of West Africa and Papua New Guinea. European journal of clinical pharmacology. 2006 Apr;62(4):267–75.

43. Lang T, Klein K, Richter T, Zibat A, Kerb R, Eichelbaum M, et al. Multiple novel nonsynonymous CYP2B6 gene polymorphisms in Caucasians: demonstration of phenotypic null alleles. The Journal of pharmacology and experimental therapeutics. 2004 Oct;311(1):34–43.

44. Rodríguez-Nóvoa S, Barreiro P, Jiménez-Nácher I, Soriano V. Overview of the pharmacogenetics of HIV therapy. The pharmacogenomics journal. 2006;6(4):234–45.

45. Arab-Alameddine M, Di Iulio J, Buclin T, Rotger M, Lubomirov R, Cavassini M, et al. Pharmacogenetics-based population pharmacokinetic analysis of efavirenz in HIV-1-infected individuals. Clinical pharmacology and therapeutics. 2009 May;85(5):485–94.

46. Kwara A, Lartey M, Sagoe KWC, Kenu E, Court MH. CYP2B6, CYP2A6 and UGT2B7 genetic polymorphisms are predictors of efavirenz mid-dose concentration in HIV-infected patients. AIDS. 2009 Oct 23;23(16):2101–6.

47. Pozniak AL, Miller RF, Lipman MC, Freedman AR, Ormerod LP, Johnson MA, et al. BHIVA treatment guidelines for tuberculosis (TB)/HIV infection 2005. HIV Med. 2005;6 Suppl 2:62–83.

48. Backman JT, Granfors MT, Neuvonen PJ. Rifampicin is only a weak inducer of CYP1A2-mediated presystemic and systemic metabolism: studies with tizanidine and caffeine. Eur J Clin Pharmacol. 2006;62(6):451–61.

49. Huang SM, Temple R, Throckmorton DC, Lesko LJ. Drug interaction studies: study design, data analysis, and implications for dosing and labeling. Clin Pharmacol Ther. 2007/01/30 ed. 2007;81(2):298–304.

50. Lopez-Cortes LF, Ruiz-Valderas R, Viciana P, Alarcon-Gonzalez A, Gomez-Mateos J, Leon-Jimenez E, et al. Pharmacokinetic interactions between efavirenz and rifampicin in HIV-infected patients with tuberculosis. Clin Pharmacokinet. 2002;41(9):681–90.

51. Centers for Disease Control and Prevention. Managing Drug Interactions in the Treatment of HIV-Related Tuberculosis [Internet]. Available from URL: http://www.cdc.gov/tb/TB_HIV_Drugs/default.htm; 2007 [cited 2012 Oct 22]. Available from: http://www.cdc.gov/tb/publications/guidelines/tb_hiv_drugs/PDF/tbhiv.pdf

52. DiGiacinto JL, Chan-Tack KM, Robertson SM, Reynolds KS, Struble K a. Are literature references sufficient for dose recommendations? An FDA case study of efavirenz and rifampin. Journal of clinical pharmacology. 2008 Apr;48(4):518–23.

53. Gengiah TN, Holford NHG, Botha JH, Gray AL, Naidoo K, Abdool Karim SS. The influence of tuberculosis treatment on efavirenz clearance in patients co-infected with HIV and tuberculosis. European journal of clinical pharmacology. 2011 Nov 23;

54. Wire MB, Ballow C, Preston SL, Hendrix CW, Piliero PJ, Lou Y, et al. Pharmacokinetics and safety of GW433908 and ritonavir, with and without efavirenz, in healthy volunteers. AIDS. 2004 Apr 9;18(6):897–907.

55. Ma Q, Forrest A, Rosenkranz SL, Para MF, Yarasheski KE, Reichman RC, et al. Pharmacokinetic interaction between efavirenz and dual protease inhibitors in healthy volunteers. Biopharmaceutics & drug disposition. 2008 Mar;29(2):91–101.

56. Krishna G, Moton A, Ma L, Martinho M, Seiberling M, McLeod J. Effects of oral posaconazole on the pharmacokinetics of atazanavir alone and with ritonavir or with efavirenz in healthy adult volunteers. Journal of acquired immune deficiency syndromes (1999). 2009 Aug 1;51(4):437–44.

57. Soon GH, Shen P, Yong E-L, Pham P, Flexner C, Lee L. Pharmacokinetics of darunavir at 900 milligrams and ritonavir at 100 milligrams once daily when coadministered with efavirenz at 600 milligrams once daily in healthy volunteers. Antimicrobial agents and chemotherapy. 2010 Jul;54(7):2775–80.

58. Dooley KE, Park J-G, Swindells S, Allen R, Haas DW, Cramer Y, et al. Safety, tolerability, and pharmacokinetic interactions of the antituberculous agent TMC207 (bedaquiline) with efavirenz in healthy volunteers: AIDS Clinical Trials Group Study A5267. Journal of acquired immune deficiency syndromes. 2012 Apr 15;59(5):455–62.

59. Oswald S, Meyer zu Schwabedissen HE, Nassif A, Modess C, Desta Z, Ogburn ET, et al. Impact of efavirenz on intestinal metabolism and transport: insights from an interaction study with ezetimibe in healthy volunteers. Clinical pharmacology and therapeutics. 2012 Mar;91(3):506–13.

60. Jetter A, Fätkenheuer G, Frank D, Klaassen T, Seeringer A, Doroshyenko O, et al. Do activities of cytochrome P450 (CYP)3A, CYP2D6 and P-glycoprotein differ between healthy volunteers and HIV-infected patients? Antiviral therapy. 2010 Jan;15(7):975–83.

61. Jones AEE, Brown KCC, Werner REE, Gotzkowsky K, Gaedigk A, Blake M, et al. Variability in drug metabolizing enzyme activity in HIV-infected patients. European journal of clinical pharmacology. 2010;66(5):475–85.

62. Morgan ET. Impact of infectious and inflammatory disease on cytochrome P450-mediated drug metabolism and pharmacokinetics. Clinical pharmacology and therapeutics. 2009 Apr;85(4):434–8.

63. Morgan ET, Goralski KB, Piquette-miller M, Renton KW, Robertson GR, Chaluvadi MR, et al. Regulation of Drug-Metabolizing Enzymes and Transporters in Infection, Inflammation, and Cancer. Pharmacology. 2008;36(2):205–16.

64. Aitken AE, Morgan ET. Gene-specific effects of inflammatory cytokines on cytochrome P450 2C, 2B6 and 3A4 mRNA levels in human hepatocytes. Drug Metab Disposition. 2007/06/20 ed. 2007;35(9):1687–93.

65. Welage LS, Carver PL, Revankar S, Pierson C, Kauffman CA. Alterations in gastric acidity in patients infected with human immunodeficiency virus. Clin Infect Dis. 1995;21(6):1431–8.

66. Zhu L, Persson A, Mahnke L, Eley T, Li T, Xu X, et al. Effect of low-dose omeprazole (20 mg daily) on the pharmacokinetics of multiple-dose atazanavir with ritonavir in healthy subjects. Journal of clinical pharmacology. 2011 Mar;51(3):368–77.

67. Brenchley JM, Douek DC. HIV infection and the gastrointestinal immune system. Mucosal immunology. 2008 Jan;1(1):23–30.

68. Cummins AG, LaBrooy JT, Stanley DP, Rowland R, Shearman DJ. Quantitative histological study of enteropathy associated with HIV infection. British Medical Journal. 1990;31(3):317.

69. Laine L, Garcia F, McGilligan K, Malinko A, Sinatra FR, Thomas DW. Protein-losing enteropathy and hypoalbuminemia in AIDS. AIDS. 1993/06/01 ed. 1993;7(6):837–40.

70. Boffito M, Back DJ, Blaschke TF, Rowland M, Bertz R, Gerber JG, et al. Protein binding in antiretroviral therapies. AIDS research and human retroviruses. 2003;19(9):825–35.

71. Marzolini C, Telenti A, Decosterd L a, Greub G, Biollaz J, Buclin T. Efavirenz plasma levels can predict treatment failure and central nervous system side effects in HIV-1-infected patients. AIDS. 2001 Jan 5;15(1):71–5.

72. Csajka C, Marzolini C, Fattinger K, Decosterd LA, Fellay J, Telenti A, et al. Population pharmacokinetics and effects of efavirenz in patients with human immunodeficiency virus infection. Clin Pharmacol Ther. 2003/01/25 ed. 2003;73(1):20–30.

73. Ståhle L, Moberg L, Svensson J, Sönnerborg A. Efavirenz plasma concentrations in HIV-infected patients: inter-and intraindividual variability and clinical effects. Therapeutic drug. 2004;26(3):267–70.

74. Leth FV, Kappelhoff BS, Johnson D, Losso MH, Boron-Kaczmarska A, Saag MS, et al. Pharmacokinetic parameters of nevirapine and efavirenz in relation to antiretroviral efficacy. AIDS research and human retroviruses. 2006 Mar;22(3):232–9.

75. Dickinson L, Boffito M, Back D, Waters L, Else L, Davies G, et al. Population pharmacokinetics of ritonavir-boosted atazanavir in HIV-infected patients and healthy volunteers. The Journal of antimicrobial chemotherapy. 2009 Jun;63(6):1233–43.

76. Le Tiec C, Barrail A, Goujard C, Taburet A-M. Clinical pharmacokinetics and summary of efficacy and tolerability of atazanavir. Clinical pharmacokinetics. 2005 Jan;44(10):1035–50.

77. Bristol-Myers Squibb. Reytaz label [Internet]. 2012 [cited 2012 Oct 15]. Available from: http://www.accessdata.fda.gov/drugsatfda_docs/label/2012/021567s028lbl.pdf

78. Bentué-Ferrer D, Arvieux C, Tribut O, Ruffault A, Bellissant E. Clinical pharmacology, efficacy and safety of atazanavir: a review. Expert opinion on drug metabolism & toxicology. 2009 Nov;5(11):1455–68.

79. Dancygier H. Clinical Hepatology. Clinical Hepatology. Berlin, Heidelberg: Springer Berlin Heidelberg; 2010. p. 103–25.

80. Cui Y, König J, Leier I, Buchholz U, Keppler D. Hepatic uptake of bilirubin and its conjugates by the human organic anion transporter SLC21A6. Journal of Biological Chemistry. 2001;276(13):9626.

81. Mediavilla MG, Pascolo L, Rodriguez JV, Guibert EE, Ostrow JD, Tiribelli C. Uptake of [3H] bilirubin in freshly isolated rat hepatocytes: role of free bilirubin concentration. FEBS letters. 1999;463(1-2):143–5.

82. Bosma PJ, Seppen J, Goldhoorn B, Bakker C, Oude Elferink RP, Chowdhury JR, et al. Bilirubin UDP-glucuronosyltransferase 1 is the only relevant bilirubin glucuronidating isoform in man. The Journal of biological chemistry. 1994 Jul 8;269(27):17960–4.

83. Ehmer U, Kalthoff S, Fakundiny B. Gilbert syndrome redefined: A complex genetic haplotype influences the regulation of glucuronidation. Hepatology. 2011;55(6):1912–21.

84. Zhang D, Chando TJ, Everett DW, Patten CJ, Dehal SS, Humphreys WG. In vitro inhibition of UDP glucuronosyltransferases by atazanavir and other HIV protease inhibitors and the relationship of this property to in vivo bilirubin glucuronidation. Drug Metabolism and Disposition. 2005 Nov;33(11):1729–39.

85. Rodríguez-Nóvoa S, Martín-Carbonero L, Barreiro P, González-Pardo G, Jiménez-Nácher I, González-Lahoz J, et al. Genetic factors influencing atazanavir plasma concentrations and the risk of severe hyperbilirubinemia. AIDS. 2007;21(1):41.

86. Monaghan G, Ryan M, Hume R, Burchell B, Seddon R. Genetic variation in bilirubin UDP-glucuronosyltransferase gene promoter and Gilbert's syndrome. The Lancet. 1996;347(9001):578–81.

87. Annaert P, Ye ZW, Stieger B, Augustijns P. Interaction of HIV protease inhibitors with OATP1B1, 1B3, and 2B1. Xenobiotica. 2010;40(3):163–76.

88. Hartkoorn RC, Kwan WS, Shallcross V, Chaikan A, Liptrott N, Egan D, et al. HIV protease inhibitors are substrates for OATP1A2, OATP1B1 and

OATP1B3 and lopinavir plasma concentrations are influenced by SLCO1B1 polymorphisms. Pharmacogenetics and genomics. 2010;20(2):112.

89. Campbell SD, de Morais SM, Xu JJ. Inhibition of human organic anion transporting polypeptide OATP 1B1 as a mechanism of drug-induced hyperbilirubinemia. Chemico-biological interactions. 2004;150(2):179–87.

90. Requena DGD, Bonora S, Cavecchia I, Veronese L, Garbo AD. Atazanavir (ATV) C trough is associated with efficacy and safety at 24 weeks : definition of therapeutic range. 6th International Workshop on Clinical Pharmacology of HIV therapy Quebec. 2005;

91. Karlström O, Josephson F, Sönnerborg A. Early virologic rebound in a pilot trial of ritonavir-boosted atazanavir as maintenance monotherapy. Journal of acquired immune deficiency syndromes. 2007 Apr 1;44(4):417–22.

92. Petersen K, Riddle M, Jones L, Furtek K, Christensen A, Tasker S, et al. Use of bilirubin as a marker of adherence to atazanavir-based antiretroviral therapy. AIDS. 2005;19(15):1700–2.

93. Edén A, Andersson LM, Andersson Ö, Flamholc L, Josephson F, Nilsson S, et al. Differential Effects of Efavirenz, Lopinavir/r, and Atazanavir/r on the Initial Viral Decay Rate in Treatment Naïve HIV-1–Infected Patients. AIDS research and human retroviruses. 2010;26(5):533–40.

94. Josephson F, Andersson MC, Flamholc L, Gisslen M, Hagberg L, Ormaasen V, et al. The relation between treatment outcome and efavirenz, atazanavir or lopinavir exposure in the NORTHIV trial of treatment-naive HIV-1 infected patients. Eur J Clin Pharmacol. 2009/12/08 ed. 2009;66:349–57.

95. Morello J, Alvarez E, Cuenca L, Vispo E, González-Lahoz J, Soriano V, et al. Use of serum bilirubin levels as surrogate marker of early virological response to atazanavir-based antiretroviral therapy. AIDS research and human retroviruses. 2011 Oct;27(10):1043–5.

96. Ray JE, Marriott D, Bloch MT, McLachlan AJ. Therapeutic drug monitoring of atazanavir: surveillance of pharmacotherapy in the clinic. British journal of clinical pharmacology. 2005 Sep;60(3):291–9.

97. Suryawanshi S, Zhang L, Pfister M, Meibohm B. The current role of model-based drug development. Expert Opinion on Drug Discovery. 2010 Apr;5(4):311–21.

98. Goldberger MJ, Singh N, Allerheiligen S, Allerheiligan S, Gobburu JVS, Lalonde R, et al. ASCPT Task Force for advancing pharmacometrics and in-

tegration into drug development. Clinical pharmacology and therapeutics. American Society of Clinical Pharmacology and Therapeutics; 2010 Aug;88(2):158–61.

99. Lee JY, Garnett CE, Gobburu JVS, Bhattaram VA, Brar S, Earp JC, et al. Impact of Pharmacometric Analyses on New Drug Approval and Labelling Decisions: A Review of 198 Submissions Between 2000 and 2008. Clinical Pharmacokinetics. 2011;50(10):0–627.

100. Pillai GC, Mentré F, Steimer J-L. Non-linear mixed effects modeling - from methodology and software development to driving implementation in drug development science. Journal of pharmacokinetics and pharmacodynamics. 2005 Apr;32(2):161–83.

101. Sheiner LB, Rosenberg B, Marathe VV. Estimation of population characteristics of pharmacokinetic parameters from routine clinical data. Journal of pharmacokinetics and biopharmaceutics. 1977 Oct;5(5):445–79.

102. Beal SL, Sheiner LB. The NONMEM system. American Statistician. 1980;34:118–9.

103. Duffull SB, Wright DFB, Winter HR. Interpreting population pharmacokinetic-pharmacodynamic analyses - a clinical viewpoint. British journal of clinical pharmacology. 2011 Jun;71(6):807–14.

104. Wählby U, Thomson AH, Milligan PA, Karlsson MO. Models for time-varying covariates in population pharmacokinetic-pharmacodynamic analysis. British journal of clinical pharmacology. 2004;58(4):367–77.

105. Karlsson MO, Sheiner LB. The importance of modeling interoccasion variability in population pharmacokinetic analyses. Journal of pharmacokinetics and biopharmaceutics. 1993 Dec;21(6):735–50.

106. Jacqmin P, Snoeck E. Clinical Trial Simulations: Viral Dynamic Modeling and Simulations in HIV and Hepatitis C. 1st ed. Kimko HHC, Peck CC, editors. World. New York, NY: Springer New York; 2011. p. 227–50.

107. Rosario MC, Poland B, Sullivan J, Westby M, van der Ryst E. A pharmacokinetic-pharmacodynamic model to optimize the phase IIa development program of maraviroc. Journal of acquired immune deficiency syndromes. 2006 Jun;42(2):183–91.

108. Rosario MC, Jacqmin P, Dorr P, van der Ryst E, Hitchcock C. A pharmacokinetic-pharmacodynamic disease model to predict in vivo antiviral activity

of maraviroc. Clinical pharmacology and therapeutics. 2005 Nov;78(5):508–19.

109. Röshammar D, Simonsson USH, Ekvall H, Flamholc L, Ormaasen V, Vesterbacka J, et al. Non-linear mixed effects modeling of antiretroviral drug response after administration of lopinavir, atazanavir and efavirenz containing regimens to treatment-naïve HIV-1 infected patients. Journal of pharmacokinetics and pharmacodynamics. 2011 Dec 2;38(6):727–42.

110. Rostami-Hodjegan A, Tucker GT. Simulation and prediction of in vivo drug metabolism in human populations from in vitro data. Nat Rev Drug Discov. 2007/02/03 ed. 2007;6(2):140–8.

111. Jamei M, Dickinson L, Rostami-Hodjegan A. A Framework for Assessing Inter-individual Variability in Pharmacokinetics Using Virtual Human Populations and Integrating General Knowledge of Physical Chemistry, Biology, Anatomy, Physiology and Genetics: A Tale of "Bottom-Up" vs "Top-Down" Recognition. Drug Metabolism and Pharmacokinetics. 2009;24(1):53–75.

112. Rowland M, Peck C, Tucker G. Physiologically-based pharmacokinetics in drug development and regulatory science. Annual Review of Pharmacology and Toxicology. Annual Reviews; 2011;51(September):45–73.

113. Pang K, Rowland M. Hepatic Clearance of Drugs . I . Theoretical Considerations of a " Well-Stirred " Model and a " Parallel Tube " Model . Influence of Hepatic Blood Flow , Plasma and Blood Cell Binding , and the Hepatocellular Enzymatic Activity on Hepatic Drug Clearance. Journal of pharmacokinetics and biopharmaceutics. 1977;5(6):625–53.

114. Benet LZ, Zia-Amirhosseini P. Basic Principles of Pharmacokinetics. Toxicologic Pathology. 1995 Mar;23(2):115–23.

115. Rowland M, Tozer N. Clinical pharmacokinetics and pharmacodynamics concepts and applications. 4th ed. Lippincott Williams & Wilkins; 2010.

116. Lobell M, Sivarajah V. In silico prediction of aqueous solubility, human plasma protein binding and volume of distribution of compounds from calculated pK a and AlogP98 values. Molecular diversity. 2003;7:69–87.

117. Ohtani H, Barter Z, Minematsu T, Makuuchi M, Sawada Y, Rostami-Hodjegan A. Bottom-up modeling and simulation of tacrolimus clearance: prospective investigation of blood cell distribution, sex and CYP3A5 expression as covariates and assessment of study power. Biopharmaceutics & drug disposition. 2011 Dec;32(9):498–506.

118. Proctor NJ, Tucker GT, Rostami-Hodjegan A. Predicting drug clearance from recombinantly expressed CYPs: intersystem extrapolation factors. Xenobiotica. 2004/02/27 ed. 2004;34(2):151–78.

119. Barter ZE, Bayliss MK, Beaune PH, Boobis AR, Carlile DJ, Edwards RJ, et al. Scaling Factors for the Extrapolation of In Vivo Metabolic Drug Clearance From In Vitro Data: Reaching a Consensus on Values of Human Microsomal Protein and Hepatocellularity Per Gram of Liver. Current Drug Metabolism. 2007 Jan 1;8(1):33–45.

120. Barter ZE, Chowdry JE, Harlow JR, Snawder JE, Lipscomb JC, Rostami-Hodjegan A. Covariation of human microsomal protein per gram of liver with age: absence of influence of operator and sample storage may justify interlaboratory data pooling. Drug Metabolism and Disposition. 2008 Dec;36(12):2405–9.

121. Johnson TN, Tucker GT, Tanner MS, Rostami-Hodjegan A. Changes in liver volume from birth to adulthood: a meta-analysis. Liver transplantation. 2005 Dec;11(12):1481–93.

122. Barter ZE. Determination of hepatic scaling factors and their inter-individual variability for use in the prediction of human metabolic clearance. Ph.D. Thesis, School of Medicine and Biomedical Sciences, The University of Sheffield; 2006.

123. Ma Q, Lu AYH. Origins of individual variability in P4501A induction. Chemical research in toxicology. 2003 Mar;16(3):249–60.

124. Plowchalk DR, Rowland Yeo K. Prediction of drug clearance in a smoking population: modeling the impact of variable cigarette consumption on the induction of CYP1A2. European journal of clinical pharmacology. 2012 Jun;68(6):951–60.

125. Gobburu JVS. Pharmacometrics 2020. Journal of clinical pharmacology. 2010 Sep;50(9 Suppl):151S–157S.

126. Jauslin PM, Silber HE, Frey N, Gieschke R, Simonsson USH, Jorga K, et al. An integrated glucose-insulin model to describe oral glucose tolerance test data in type 2 diabetics. Journal of clinical pharmacology. 2007 Oct;47(10):1244–55.

127. Karlsson MO, Schoemaker RC, Kemp B, Cohen a F, van Gerven JM, Tuk B, et al. A pharmacodynamic Markov mixed-effects model for the effect of temazepam on sleep. Clinical pharmacology and therapeutics. 2000 Aug;68(2):175–88.

128. Fätkenheuer G, Staszewski S, Plettenburg A, Hackman F, Layton G, McFadyen L, et al. Activity, pharmacokinetics and safety of lersivirine (UK-453,061), a next-generation nonnucleoside reverse transcriptase inhibitor, during 7-day monotherapy in HIV-1-infected patients. AIDS. 2009 Oct 23;23(16):2115–22.

129. Moyle G, Boffito M, Stoehr A, Rieger A, Shen Z, Manhard K, et al. Phase 2a randomized controlled trial of short-term activity, safety, and pharmacokinetics of a novel nonnucleoside reverse transcriptase inhibitor, RDEA806, in HIV-1-positive, antiretroviral-naive subjects. Antimicrobial agents and chemotherapy. 2010 Aug;54(8):3170–8.

130. Min S, Sloan L, DeJesus E, Hawkins T, McCurdy L, Song I, et al. Antiviral activity, safety, and pharmacokinetics/pharmacodynamics of dolutegravir as 10-day monotherapy in HIV-1-infected adults. AIDS. 2011 Sep 10;25(14):1737–45.

131. Goebel F, Yakovlev A, Pozniak AL, Vinogradova E, Boogaerts G, Hoetelmans R, et al. Short-term antiviral activity of TMC278--a novel NNRTI--in treatment-naive HIV-1-infected subjects. AIDS. 2006 Aug 22;20(13):1721–6.

132. Fätkenheuer G, Pozniak AL, Johnson M a, Plettenberg A, Staszewski S, Hoepelman AIM, et al. Efficacy of short-term monotherapy with maraviroc, a new CCR5 antagonist, in patients infected with HIV-1. Nature medicine. 2005 Nov;11(11):1170–2.

133. EMEA. Guideline on the clinical development of medicinal products for the treatment of HIV infection [Internet]. EMEA. 2009 [cited 2012 Aug 8]. Available from: http://www.ema.europa.eu/docs/en_GB/document_library/Scientific_guideline/2009/09/WC500003399.pdf

134. Jonsson EN, Sheiner LB. More efficient clinical trials through use of scientific model-based statistical tests. Clinical pharmacology and therapeutics. 2002 Dec;72(6):603–14.

135. Sheiner LB. Is intent to treat analysis always (ever) enough? British journal of clinical pharmacology. 2002;54(2):203–11.

136. Wählby U, Bouw MR, Jonsson EN, Karlsson MO. Assessment of type I error rates for the statistical sub-model in NONMEM. Journal of pharmacokinetics and pharmacodynamics. 2002 Jun;29(3):251–69.

137. Wählby U, Jonsson ENN, Karlsson MO. Assessment of actual significance levels for covariate effects in NONMEM. Journal of pharmacokinetics and pharmacodynamics. Springer; 2001 Jun;28(3):231–52.

138. Vong C, Bergstrand M, Nyberg J, Karlsson MO. Rapid sample size calculations for a defined likelihood ratio test-based power in mixed-effects models. The AAPS journal. 2012 Jun 17;14(2):176–86.

139. Karlsson KE. Benefits of Pharmacometric Model-Based Design and Analysis of Clinical Trials. Acta Universitatis Upsaliensis, Uppsala. ISSN 1651-6192; 2010. p. 1–71.

140. Jamei M, Marciniak S, Feng K, Barnett A, Tucker G, Rostami-Hodjegan A. The Simcyp population-based ADME simulator. Expert opinion on drug metabolism & toxicology. 2009 Feb;5(2):211–23.

141. Faucette SR, Wang H, Hamilton G a, Jolley SL, Gilbert D, Lindley C, et al. Regulation of CYP2B6 in primary human hepatocytes by prototypical inducers. Drug Metabolism and Disposition. 2004 Mar;32(3):348–58.

142. Jansson R, Bredberg U, Ashton M. Prediction of drug tissue to plasma concentration ratios using a measured volume of distribution in combination with lipophilicity. J Pharm Sci. 2007/08/29 ed. 2008;97(6):2324–39.

143. S. M. Rowe S. R. Rabel, and M. B. Maurin LGF. Physical Chemical Properties of Efavirenz. AAPS Annual Meeting and Exposition, AAPS PharmSci Supplement. 1999;

144. Balani SKK, Kauffman LRR, DeLuna FAA, Lin JHH. Nonlinear pharmacokinetics of efavirenz (DMP-266), a potent HIV-1 reverse transcriptase inhibitor, in rats and monkeys. Drug metabolism and disposition. 1999/01/12 ed. ASPET; 1999;27(1):41–5.

145. Takano R, Sugano K, Higashida A, Hayashi Y, Machida M, Aso Y, et al. Oral absorption of poorly water-soluble drugs: computer simulation of fraction absorbed in humans from a miniscale dissolution test. Pharm Res. 2006/05/23 ed. 2006;23(6):1144–56.

146. Austin RP, Barton P, Cockroft SL, Wenlock MC, Riley RJ. The influence of nonspecific microsomal binding on apparent intrinsic clearance, and its prediction from physicochemical properties. Drug Metab Disposition. 2002/11/16 ed. 2002 Dec 1;30(12):1497–503.

147. Shou M, Hayashi M, Pan Y, Xu Y, Morrissey K, Xu L, et al. Modeling, prediction, and in vitro in vivo correlation of CYP3A4 induction. Drug Metab Disposition. 2008/08/02 ed. 2008;36(11):2355–70.

148. Bélanger AS, Caron P, Harvey M, Zimmerman PAA, Mehlotra RKK, Guillemette C, et al. Glucuronidation of the antiretroviral drug efavirenz by UGT2B7 and an in vitro investigation of drug-drug interaction with zidovudine. Drug Metabolism and Disposition. 2009/06/03 ed. ASPET; 2009;37(9):1793.

149. Anderson BJ, Holford NHG. Mechanism-based concepts of size and maturity in pharmacokinetics. Pharmacology and Toxicology. 2008;48(1):303.

150. Savic RM, Jonker DM, Kerbusch T, Karlsson MO. Implementation of a transit compartment model for describing drug absorption in pharmacokinetic studies. J Pharmacokinet Pharmacodyn. 2007/07/27 ed. 2007;34(5):711–26.

151. Lindbom L, Pihlgren P, Jonsson EN. PsN-Toolkit--a collection of computer intensive statistical methods for non-linear mixed effect modeling using NONMEM. Comput Methods Programs Biomed. 2005/07/19 ed. 2005;79(3):241–257 [http://psn.sourceforge.net/].

152. Beal S, Sheiner LB, Boeckmann A, Bauer, R J. NONMEM users guides (1989-2009). ICON Development Solutions, Ellicott City MD, USA, 2009.

153. Wilkins JJ. NONMEMory: a run management tool for NONMEM. Computer Methods and Programs in Biomedicine. 2005;78(3):259–67.

154. Jonsson EN, Karlsson MO. Xpose--an S-PLUS based population pharmacokinetic/pharmacodynamic model building aid for NONMEM. Comput Methods Programs Biomed. 1999/04/09 ed. 1998;58(1):51–64 [http://xpose.sourceforge.net/].

155. Berk PD, Howe RB, Bloomer JR, Berlin NI. Studies of bilirubin kinetics in normal adults. Journal of Clinical Investigation. 1969;48(11):2176.

156. Macey R, Oster G, Zahnley T, University of California. Berkeley Madonna User's Guide Version 8.0.2 [Internet]. 2009 [cited 2012 Sep 9]. Available from: http://www.berkeleymadonna.com/BM User's Guide 8.0.2.pdf

157. Keizer RJ, van Benten M, Beijnen JH, Schellens JH, Huitema AD. Piraña and PCluster: a modeling environment and cluster infrastructure for NONMEM. Computer Methods and Programs in Biomedicine. Elsevier Ireland Ltd; 2011;101(1):72–79 [http://pirana–software.com/].

158. Savic RM, Barrail-Tran A, Duval X, Nembot G, Panhard X, Descamps D, et al. Effect of Adherence as Measured by MEMS, Ritonavir Boosting, and CYP3A5 Genotype on Atazanavir Pharmacokinetics in Treatment-Naive HIV-Infected Patients. Clinical pharmacology and therapeutics. 2012 Oct 3;

159. Lindbom L, Ribbing J, Jonsson EN. Perl-speaks-NONMEM (PsN)--a Perl module for NONMEM related programming. Computer methods and programs in biomedicine. 2004;75(2):85–94 [http://psn.sourceforge.net/].

160. Matteelli A, Regazzi M, Villani P. Multiple-dose pharmacokinetics of efavirenz with and without the use of rifampicin in HIV-positive patients. Current HIV Research. 2007;5(3):349–53.

161. Sharma A, Jusko WJ. Characteristics of indirect pharmacodynamic models and applications to clinical drug responses. British journal of clinical pharmacology. 1998;45(3):229–39.

162. Schönnesson LN, Ross MW, Williams M. The HIV Medication Self-Reported Nonadherence Reasons (SNAR) Index and its underlying psychological dimensions. AIDS and behavior. 2004 Sep;8(3):293–301.

163. Slusher T, Angyo I, Bode-Thomas F. Transcutaneous bilirubin measurements and serum total bilirubin levels in indigenous African infants. Pediatrics. 2004;113(6):1636–41.